

The BZR1-EDS1 module regulates plant growth-defense coordination

Guang Qi^{1,2}, Huan Chen^{2,3}, Dian Wang⁴, Hongyuan Zheng¹, Xianfeng Tang⁵, Zhengzheng Guo¹, Jiayu Cheng¹, Jian Chen^{2,3}, Yiping Wang⁵, Ming-yi Bai⁶, Fengquan Liu³, Daowen Wang^{1,*} and Zheng Qing Fu^{2,*}

¹State Key Laboratory of Wheat and Maize Crop Science, College of Agronomy, and Center for Crop Genome Engineering, Henan Agricultural University, Zhengzhou 450002, China

²Department of Biological Sciences, University of South Carolina, Columbia, SC 29208, USA

³Institute of Plant Protection, Jiangsu Academy of Agricultural Sciences, Nanjing, 210014, China

⁴College of Agronomy, Qingdao Agricultural University, Qingdao 266109, China

⁵Qingdao Institute of BioEnergy and Bioprocess Technology, Chinese Academy of Sciences, Qingdao 266109, China

⁶Key Laboratory of Plant Development and Environment Adaptation Biology, Ministry of Education, School of Life Sciences, Shandong University, 266237 Qingdao, China

*Correspondence: Daowen Wang (dwwang@henau.edu.cn), Zheng Qing Fu (zfu@mailbox.sc.edu)

<https://doi.org/10.1016/j.molp.2021.08.011>

ABSTRACT

Plants have developed sophisticated strategies to coordinate growth and immunity, but our understanding of the underlying mechanism remains limited. In this study, we identified a novel molecular module that regulates plant growth and defense in both compatible and incompatible infections. This module consisted of BZR1, a key transcription factor in brassinosteroid (BR) signaling, and EDS1, an essential positive regulator of plant innate immunity. We found that EDS1 interacts with BZR1 and suppresses its transcriptional activities. Consistently, upregulation of EDS1 function by a virulent *Pseudomonas syringae* strain or salicylic acid treatment inhibited BZR1-regulated expression of BR-responsive genes and BR-promoted growth. Furthermore, we showed that the cytoplasmic fraction of BZR1 positively regulates effector-triggered immunity (ETI) controlled by the TIR-NB-LRR protein RPS4, which is attenuated by BZR1's nuclear translocation. Mechanistically, cytoplasmic BZR1 facilitated AvrRps4-triggered dissociation of EDS1 and RPS4 by binding to EDS1, thus leading to efficient activation of RPS4-controlled ETI. Notably, transgenic expression of a mutant BZR1 that accumulates exclusively in the cytoplasm improved pathogen resistance without compromising plant growth. Collectively, these results shed new light on plant growth-defense coordination and reveal a previously unknown function for the cytoplasmic fraction of BZR1. The BZR1-EDS1 module may be harnessed for the simultaneous improvement of crop productivity and pathogen resistance.

Key words: brassinosteroid, BZR1, salicylic acid, EDS1, basal resistance, effector-triggered immunity, TIR-NB-LRR resistance protein, RPS4

Qi G., Chen H., Wang D., Zheng H., Tang X., Guo Z., Cheng J., Chen J., Wang Y., Bai M.-y., Liu F., Wang D., and Fu Z.Q. (2021). The BZR1-EDS1 module regulates plant growth-defense coordination. *Mol. Plant*. **14**, 1–16.

INTRODUCTION

Plants are constantly challenged by diverse pathogenic microbes in their growth environments and have therefore evolved sophisticated strategies to coordinate their growth and defense (Huot et al., 2014). It is now well accepted that excessive activation of pathogen defense incurs fitness costs to plant survival (Karasov et al., 2017). On the other hand, optimizing plant growth-defense coordination is beneficial for simultaneously improving crop productivity and immunity (Xu et al., 2017; Greene and Dong, 2018; Wang et al., 2018).

To date, two major types of plant innate immunity have been recognized: PAMP (pathogen-associated molecular pattern)-triggered immunity (PTI) and effector-triggered immunity (ETI) (Jones and Dangl, 2006). In PTI, plants sense conserved PAMPs by pattern recognition receptors on the cell surface; this induces multiple defense pathways and yields basal resistance (Bittel and Robatzek, 2007; Zhang and Zhou, 2010).

Molecular Plant

In ETI, an avirulent pathogenic effector is recognized by an intracellular nucleotide-binding leucine-rich repeat (NB-LRR) immune receptor (Caplan et al., 2008). This leads to the hypersensitive response (HR) and localized cell death, resulting in robust disease resistance by sacrificing the growth of a few cells (Cui et al., 2015). Furthermore, systemic acquired resistance (SAR) is widespread in plants. In SAR, a local infection by a pathogen immunizes the whole plant against subsequent infections by the same or unrelated microbes, and SAR is activated in both compatible and incompatible pathosystems (Fu and Dong, 2013).

Various phytohormones have been found to regulate plant defense responses, with the outcome often affecting both plant growth and defense-related processes (Pieterse et al., 2012). Pertinent to the scope of this work, progress on brassinosteroid (BR) signaling and BR regulation of pathogen defense is concisely outlined below. BR is perceived mainly by the cell surface-localized leucine-rich repeat receptor-like kinase BRI1, which triggers a sequential phosphorylation-dependent signal transduction cascade (Li and Chory, 1997; Kinoshita et al., 2005). This leads to the activation of BZR1 and its close homoeolog BES1, which then regulate the expression of thousands of BR-responsive genes (BRRGs) and downstream physiological and growth events (Wang et al., 2002; He et al., 2005; Kim and Wang, 2010). Under low BR conditions, BZR1 and BES1 are phosphorylated by active GSK3-like kinases (e.g., BIN2), resulting in their retention in the cytoplasm (He et al., 2002; Gampala et al., 2007). When BR concentration increases, the activities of BIN2 and related kinases are inhibited, and BZR1 and BES1 are dephosphorylated by protein phosphatase 2A (Tang et al., 2011). This stimulates nuclear translocation of BZR1 and BES1 and their binding to target gene promoters, thereby regulating the transcription of BRRGs (Sun et al., 2010).

Increasing evidence indicates that BR is actively involved in plant growth-defense coordination (De Bruyne et al., 2014; Yu et al., 2018; Kono and Yin, 2020; Nolan et al., 2020). BZR1 has been demonstrated to regulate plant growth-defense trade-offs (Lozano-Duran et al., 2013; Wang and Wang, 2014). Specifically, BZR1 was found to be required for suppressing PTI upon BR perception, mainly through the induction of several WRKY TF genes that negatively regulate the expression of defense-related proteins. Similarly, HBI1, a bHLH TF that functions downstream of BZR1, has been suggested to be a binary switch that mediates the trade-off between BR-promoted growth and PTI (Fan et al., 2014; Malinovsky et al., 2014). Moreover, exogenous application of the bacterial PAMP flg22 results in significant inhibition of the expression of BR biosynthetic genes (Jimenez-Gongora et al., 2015). BES1 was also found to play a positive role in PTI and mediate the antagonistic effect of BRs on JA-activated defense (Kang et al., 2015; Kono and Yin, 2020; Liao et al., 2020). Together, the available data indicate that the BR pathway is deeply involved in plant growth-defense coordination in a complex manner, which requires more effort to fully elucidate.

We therefore conducted yeast-two hybrid (Y2H) analysis with BZR1 as a bait and uncovered an interaction between BZR1 and EDS1. EDS1 is an essential positive regulator of both basal

BZR1-EDS1 regulates plant growth and defense

resistance and the ETI conditioned by the TIR-NLR (TNL) type of R protein (Feys et al., 2005; Rietz et al., 2011; Cui et al., 2017). Regulation of basal resistance by EDS1 involves the stimulation of SA biosynthesis. SA then enhances EDS1 expression through a positive feedback loop, thus leading to the amplification of the defense response both locally and systemically. Furthermore, EDS1 interacts with multiple TNL proteins, including RPS4 (Bhattacharjee et al., 2011). In the RPS4-controlled ETI, an immune receptor complex composed of RPS4 and another TNL protein, RRS1, senses the avirulent effector AvrRps4 in the nucleus (Le Roux et al., 2015; Sarris et al., 2015; Huh et al., 2017). AvrRps4 has also been shown to bind EDS1 in the cytoplasm, resulting in the dissociation of RPS4 and EDS1, another step essential for the efficient development of RPS4-controlled ETI (Bhattacharjee et al., 2011; Heidrich et al., 2011).

Considering the crucial importance of BZR1 in BR signaling and the pivotal role of EDS1 in plant innate immunity, the discovery of the BZR1-EDS1 interaction provided a valuable opportunity to more systematically analyze plant growth-defense coordination. We first examined the function of the BZR1-EDS1 interaction in basal resistance, and we found that upregulation of EDS1 decreased BZR1-regulated BRRG expression and growth owing to EDS1's binding to BZR1 and consequent inhibition of BZR1's transcriptional activities. Concomitantly, we discovered that maintenance of the cytoplasmic BZR1-EDS1 interaction was critical for RPS4-controlled ETI; it was weakened by promoting nuclear translocation of BZR1 but enhanced by increasing BZR1 accumulation in the cytoplasm. Interestingly, we found that transgenic expression of a BZR1 mutant that accumulated only in the cytoplasm enhanced pathogen resistance without disrupting plant growth. This observation, plus the finding of an analogous BZR1-EDS1 interaction in wheat plants, suggests that it may be possible to manipulate this module to refine crop productivity and pathogen resistance simultaneously in future research.

RESULTS

BZR1 interacts with EDS1 in both the cytoplasm and nucleus

At the first stage of this study, we found that BZR1 interacted with EDS1 in a Y2H test (Figure 1A). This was subsequently validated using *in vitro* pull-down assays conducted with GST-EDS1 and MBP-BZR1 fusion proteins (Figure 1B). Furthermore, we confirmed that BZR1 interacted with EDS1 in *Arabidopsis* plants by performing co-immunoprecipitation (Co-IP) assays using two types of transgenic lines, *p35S::BZR1-GFP* and *p35S::GFP*. As revealed by immunoblotting, EDS1 was consistently detected in the immunoprecipitates prepared from *p35S::BZR1-GFP* plants, but not from *p35S::GFP* plants, using a GFP-specific antibody (Figure 1C).

To investigate the subcellular locations of the BZR1-EDS1 interaction inside plant cells, we conducted bimolecular fluorescence complementation (BiFC) assays. Co-expression of BZR1-YFP^N and EDS1-YFP^C in *Arabidopsis* mesophyll protoplasts yielded strong yellow fluorescence in both the cytoplasm and the nucleus (Figure 1D). However, no fluorescence signal was detected in protoplasts transfected with control constructs (Figure 1D).

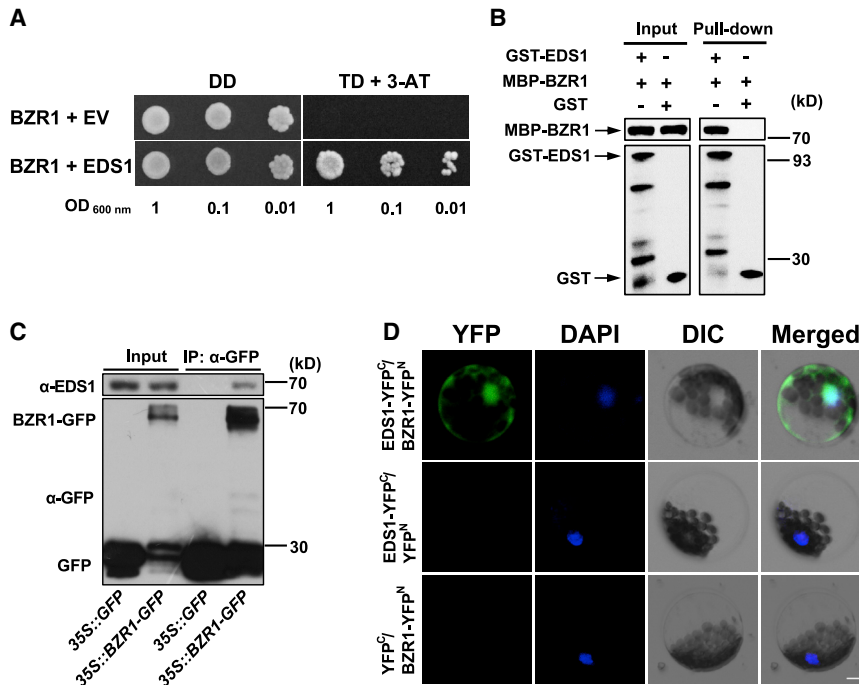


Figure 1. Interaction between BZR1 and EDS1.

(A) Interaction between BZR1 and EDS1 revealed using Y2H assays. For this assay, BZR1 and EDS1 were fused with the DNA binding (in pGBKT7) and activation (in pGADT7) domains, respectively. Transformed yeast cells, selected on a double synthetic dropout (DD) plate lacking histidine and tryptophan, were serially diluted and spotted on a triple dropout (TD) plate lacking tryptophan, leucine, and histidine but supplemented with 50 mM 3-AT. EV, empty vector.

(B) *In vitro* pull-down assay. Purified 6×His-MBP-BZR1 was incubated with GST or GST-EDS1 immobilized on MagneGST Glutathione magnetic beads. The pull-down products were separated on SDS-PAGE, followed by immunoblotting with anti-GST or anti-6×His antibodies. Arrows indicate the specific bands corresponding to 6×His-MBP-BZR1, GST-EDS1, or GST.

(C) *In planta* interaction between BZR1 and EDS1 detected using colP assays. Immunoprecipitation was performed using 10-day-old *p35S::BZR1-GFP* or *p35S::GFP* seedlings and GFP-Trap Magnetic Agarose beads. Immunoblotting was carried out using anti-GFP or anti-EDS1 antibodies. In the

p35S::BZR1-GFP input sample, a broad band of both unphosphorylated and phosphorylated BZR1-GFP was detected.

(D) BiFC assays showing the interaction between BZR1-YFP^N and EDS1-YFP^C in both the nucleus and cytoplasm of *Arabidopsis* mesophyll protoplasts. Confocal microscopy was used to image the reconstituted YFP signals, and the cell nucleus was revealed by 4',6-diamidino-2-phenylindole (DAPI) staining. Scale bar, 10 μm. The datasets displayed above are all representative of three independent experiments.

These results demonstrate that BZR1 and EDS1 interact both *in vitro* and *in vivo* and that their interaction occurs in both the cytosolic and nuclear compartments *in planta*.

Because it is well known that EDS1 forms heteromeric complexes with two signaling partners, phytoalexin-deficient 4 (PAD4) and senescence-associated protein 101 (SAG101), to confer resistance against virulent and avirulent pathogens (Feys et al., 2001), we examined whether BZR1 interacted with PAD4 or SAG101 using Y2H assays. In repeated trials, no interaction was detected between BZR1 and PAD4 or SAG101 (supplemental Figure 1A). In addition, no interaction was detected between EDS1 and the nucleus-localized bHLH transcription factor PIF4 (Bernardo-García et al., 2014), thus providing evidence for the specificity of EDS1's binding to BZR1 (supplemental Figure 1B and 1C).

EDS1 impedes the transcriptional activities of BZR1

To assess the functional significance of the BZR1-EDS1 interaction in BR signaling, we first performed transient expression assays in *Arabidopsis* mesophyll protoplasts to test the potential effects of EDS1 expression on BZR1 transcriptional activities. The promoter regions of two BZR1 target genes (*EXP8* and *SAUR15*) were each fused to the β-glucuronidase (GUS) gene as reporters, with *p35S::BZR1* and *p35S::EDS1* as effector constructs (Figure 2A). According to previous reports, *EXP8* and *SAUR15* are the BRRGs positively regulated by BZR1 (Tian et al., 2018). As anticipated, BZR1 expression significantly increased the promoter activities of *EXP8* and *SAUR15* (Figure 2B). However, co-expression of EDS1 substantially reduced the positive effects of BZR1 on the promoter activities of *EXP8* and *SAUR15* (Figure 2B). *DWF4* and *BR6OX* are two

BZR1-repressed target genes (He et al., 2005). Using similar assays, we found that EDS1 alleviated BZR1's suppression of *DWF4* and *BR6OX* promoter activities (supplemental Figure 2A and 2B).

Using *EXP8* and *SAUR15* as representatives, we next examined whether the binding of BZR1 to BRRG promoter regions was affected by EDS1 using electrophoretic mobility shift assays. In repeated EMSA assays, binding of BZR1 to the BR-responsive elements BRRE (CGTGT/CG) or E-box (CANNTG) (He et al., 2005; Yu et al., 2011), which are present in the promoter regions of *EXP8* and *SAUR15*, was quantitatively decreased by increasing amounts of EDS1 without or with the presence of PAD4 and SAG101. This phenomenon was not observed for the controls (MBP or GST-GUS) (Figure 2C and 2D and supplemental Figure 3).

To verify whether EDS1 interferes with BZR1's binding to its target promoters *in planta*, we carried out chromatin immunoprecipitation quantitative PCR (ChIP-qPCR) assays using the transgenic line *pBZR1::bzm1-1D-CFP* (mx3) (Zhang et al., 2013) developed in the wild-type (WT) Col-0 or EDS1 mutant (*eds1-2*) background, i.e., *pBZR1::bzm1-1D-CFP/Col-0* and *pBZR1::bzm1-1D-CFP/eds1-2*. A previous study has shown that *bzm1-1D* is a dominant mutant of BZR1 caused by a proline to leucine substitution in the PEST domain, and *bzm1-1D* shows elevated accumulation in both the cytoplasm and the nucleus (Wang et al., 2002). In *pBZR1::bzm1-1D-CFP* plants, a *bzm1-1D-CFP* fusion protein was expressed under the native promoter of BZR1. The ChIP-qPCR result showed significantly higher enrichment of BZR1 in the promoter regions of *EXP8* and *SAUR15* in *pBZR1::bzm1-1D-CFP/eds1-2* than in *pBZR1::bzm1-1D-CFP/Col-0* (Figure 2E),

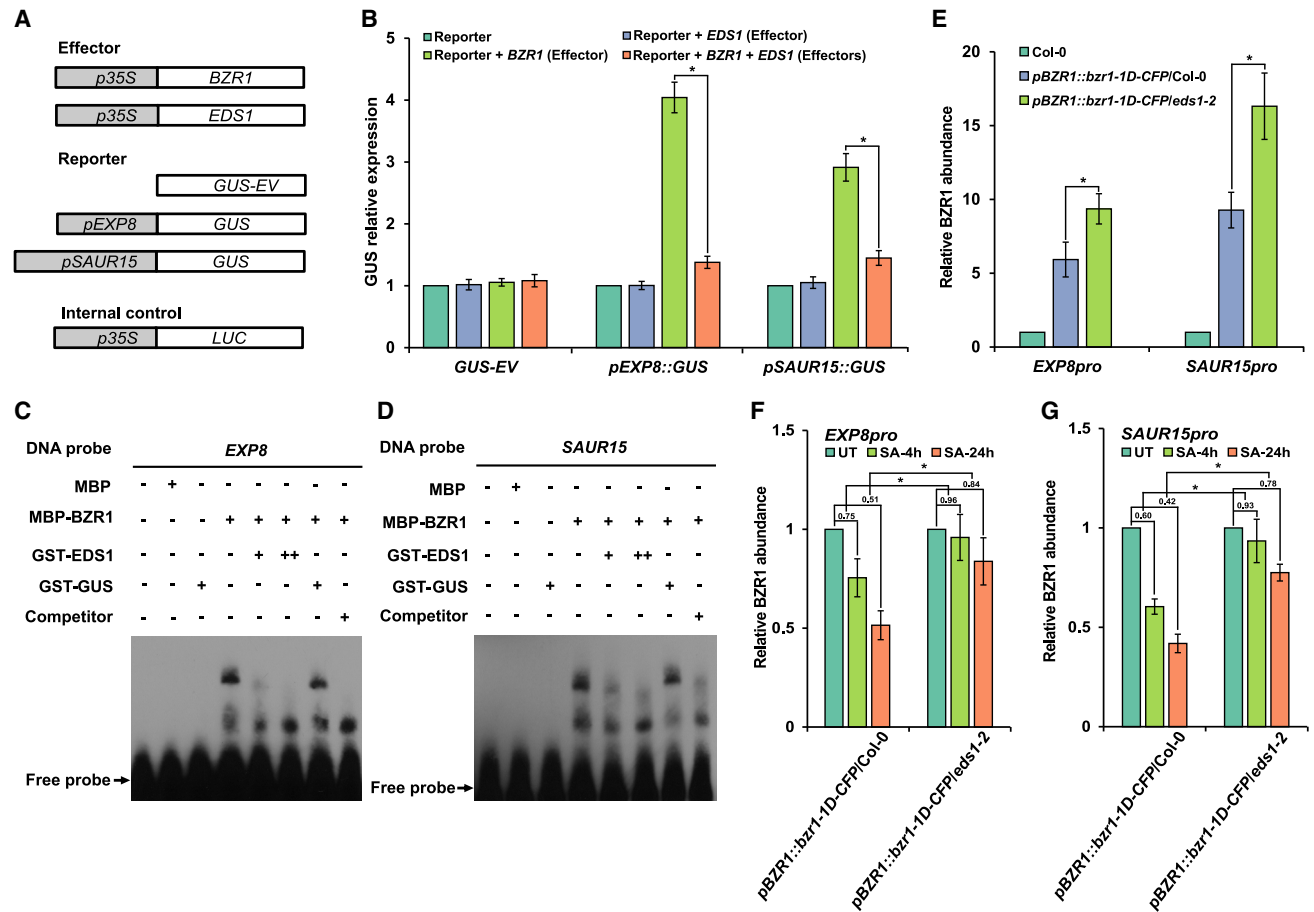


Figure 2. Inhibition of the transcriptional activities of BZR1 by EDS1.

(A and B) Transient assays showing the suppression by EDS1 of BZR1's transcriptional promotion of *EXP8* and *SAUR15* promoter-driven GUS (β -glucuronidase) expression in *Arabidopsis* mesophyll protoplasts. Various combinations of effector and reporter constructs are shown in **(A)**. The GUS expression value obtained for the protoplasts transfected with only the reporter construct was set to 1 to facilitate the comparison **(B)**. LUC expression was used as an internal control.

(C and D) Inhibition by EDS1 of BZR1's binding to *cis*-elements (BRRE and/or E-box) in the *EXP8* or *SAUR15* promoter revealed by EMSA assays. The binding of 6 \times His-MBP-BZR1 to the biotin-labeled promoter probes of *EXP8* **(C)** or *SAUR15* **(D)** was gradually reduced by increasing amounts of GST-EDS1 but not GST-GUS.

(E) Increased BZR1 binding to the *EXP8* or *SAUR15* promoter in the *eds1-2* mutant uncovered by ChIP-qPCR assays. The analysis was performed with WT Col-0 and two transgenic lines, *pBZR1::bzt1-1D-CFP/Col-0* (expressing both *bzt1-1D-CFP* fusion protein and a functional EDS1) and *pBZR1::bzt1-1D-CFP/eds1-2* (expressing *bzt1-1D-CFP* but lacking a functional EDS1). The amount of target promoter chromatin precipitated for Col-0 was set to 1 to facilitate comparison.

(F and G) EDS1-dependent suppression by SA of BZR1 binding to its target promoters (*EXP8 pro* and *SAUR15 pro*). ChIP-qPCR analysis was performed with the transgenic lines *pBZR1::bzt1-1D-CFP/Col-0* and *pBZR1::bzt1-1D-CFP/eds1-2* treated with SA for 4 and 24 h. The amount of target promoter chromatin precipitated for *pBZR1::bzt1-1D-CFP/eds1-2* was significantly higher than that for *pBZR1::bzt1-1D-CFP/Col-0*, indicating that SA-mediated suppression of BZR1 binding to its target promoters is partially dependent on the presence of a functional EDS1. UT, untreated sample. In **(B)** and **(E-G)**, error bars represent the SD of three independent experiments. * $P < 0.05$, ** $P < 0.01$ (Student's *t*-test). All experiments were repeated three times with similar results.

indicating that EDS1 dysfunction enhances BZR1 binding to the promoters of BRRGs. On the other hand, when EDS1 expression was boosted by SA treatment (supplemental Figure 4), the enrichment of BZR1 in *EXP8* and *SAUR15* promoter regions was substantially reduced in *pBZR1::bzt1-1D-CFP/Col-0*, which contained a functional EDS1, compared with that observed in *pBZR1::bzt1-1D-CFP/eds1-2*, which contained a mutated EDS1 (Figure 2F and 2G). Collectively, the above data strongly suggest that EDS1 impedes the transcriptional regulation of BRRGs (*EXP8* and *SAUR15*) by BZR1 via interfering with its transcriptional activities.

EDS1 antagonizes BR-promoted growth under normal, SA treatment, or pathogen infection conditions

Hypocotyl elongation is a typical BR-promoted growth process in *Arabidopsis*. We therefore compared the hypocotyl lengths of WT Col-0 seedlings to those of *Arabidopsis* materials whose EDS1 function was either impaired or enhanced. Relative to the WT control, hypocotyl length was significantly increased in *eds1-2* (lacking a functional EDS1) but substantially decreased in *EDS1-GFP* (overexpressing an EDS1-GFP fusion protein) (Chang et al., 2019) (Figure 3A). In agreement with this result, the average hypocotyl lengths of the *sid2* (Wildermuth et al.,

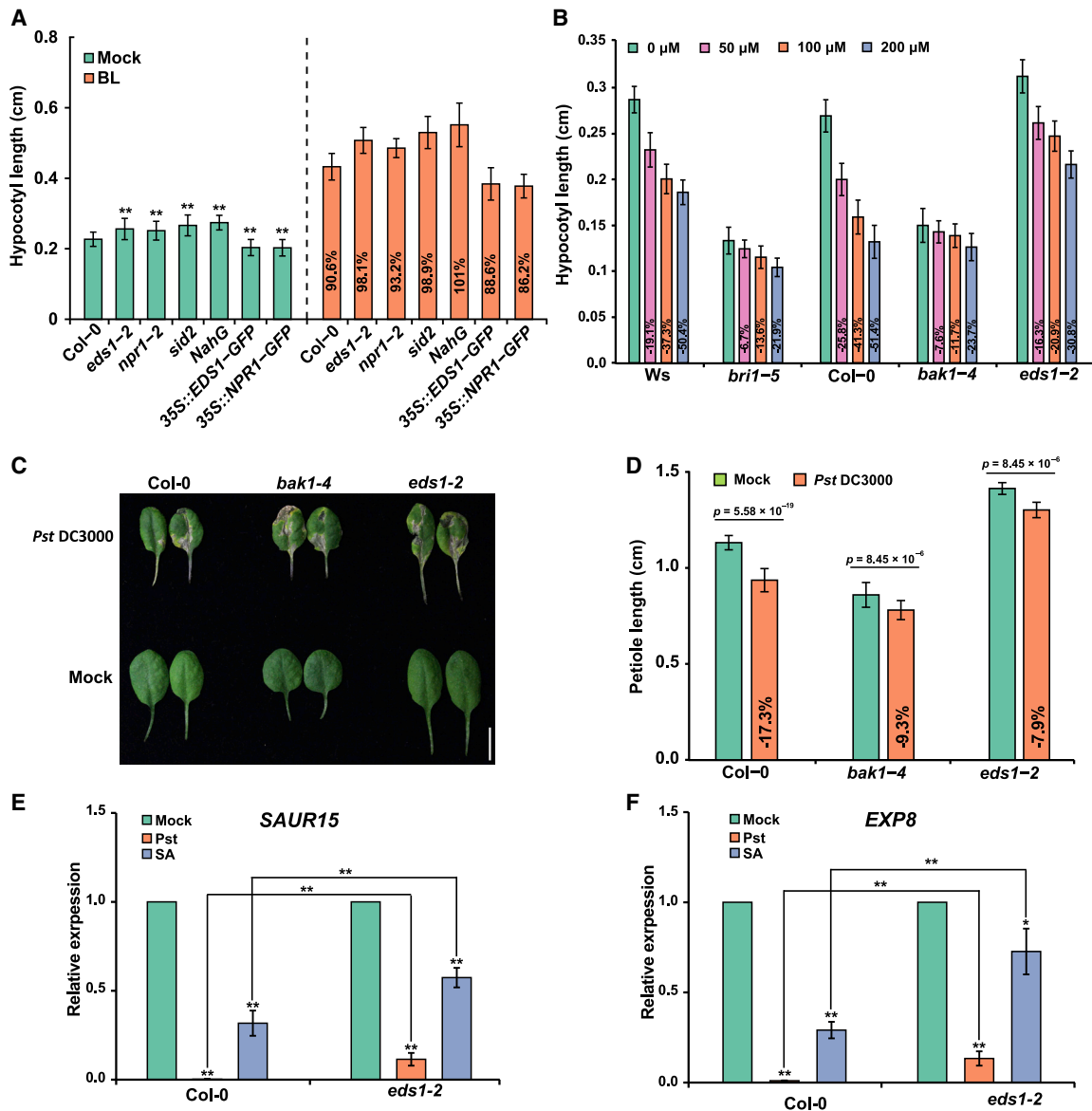


Figure 3. EDS1-dependent inhibition of BR-promoted plant growth by virulent pathogen challenge or SA treatment.

(A) Enhancement of BR-mediated hypocotyl growth in the mutants (*eds1-2* and *sid2*) or transgenic line (*NahG*) with reduced SA levels and a mutant (*npr1-2*) defective in SA perception. By contrast, BR-mediated hypocotyl growth was suppressed in transgenic lines with increased *NPR1* (*p35S::NPR1-GFP*) or EDS1 (*p35S::EDS1-GFP*) function. Seedlings were grown on $\frac{1}{2}$ MS medium with or without 10 nM BL under a 16 h light/8 h dark photoperiod for 6 days and then used for hypocotyl length measurement. Error bars, SD ($n \geq 25$ plants).

(B) Decreased SA-mediated inhibition of hypocotyl growth shown by mutants of the BR receptor (*bri1-5*) and co-receptor (*bak1-4*), as well as the *eds1-2* mutant. Seedlings were grown on $\frac{1}{2}$ MS medium containing different concentrations of SA under a 16 h light/8 h dark photoperiod for 6 days. The percentages of hypocotyl length reduction caused by the application of different concentrations of SA to WT controls (Ws and Col-0), *bri1-5*, *bak1-4*, and *eds1-2* were calculated by comparison with their respective mock controls. Error bars, SD ($n \geq 25$ plants).

(C and D) Inhibition of *Arabidopsis* petiole elongation by virulent pathogen (*Pst* DC3000) infection. Three-week-old Col-0, *bak1-4*, and *eds1-2* plants were dip inoculated with *Pst* DC3000 ($OD_{600\text{ nm}} = 0.01$). The fifth leaves were harvested and photographed at 7 dpi (C). The lengths of the petioles were measured, and the percentages of petiole length reduction caused by pathogen infection in WT Col-0, *bak1-4* lacking the functional BR co-receptor BAK1, or *eds1-2* without a functional EDS1, calculated by comparison with their respective mock controls, are shown (D). Error bars, SD ($n \geq 25$ plants).

(E and F) EDS1-dependent inhibition of BR-responsive gene expression after virulent pathogen challenge or SA treatment. Leaves of 4-week-old soil-grown WT Col-0 and *eds1-2* mutant plants were sprayed with *Pst* DC3000 ($OD_{600\text{ nm}} = 0.2$) or with 0.5 mM SA. At 24 h after the spray, total RNA was extracted and used in qRT-PCR assays to quantify the expression levels of *SAUR15* (E) and *EXP8* (F). In (A), (E), and (F), $*P < 0.05$, $**P < 0.01$ (Student's *t*-test). In (D), exact *P* values are shown above the bars. All experiments were repeated at least three times with similar results.

2001) mutant and the *NahG* (Delaney et al., 1994) transgenic line, which are deficient in SA accumulation, were much longer than that of the WT control (Figure 3A). Moreover, altering the

function of NPR1, which positively regulates SA signaling, could either enlarge the hypocotyl length (in *npr1-2* mutants with a dysfunctional NPR1) or reduce it (in *NPR1-GFP* plants

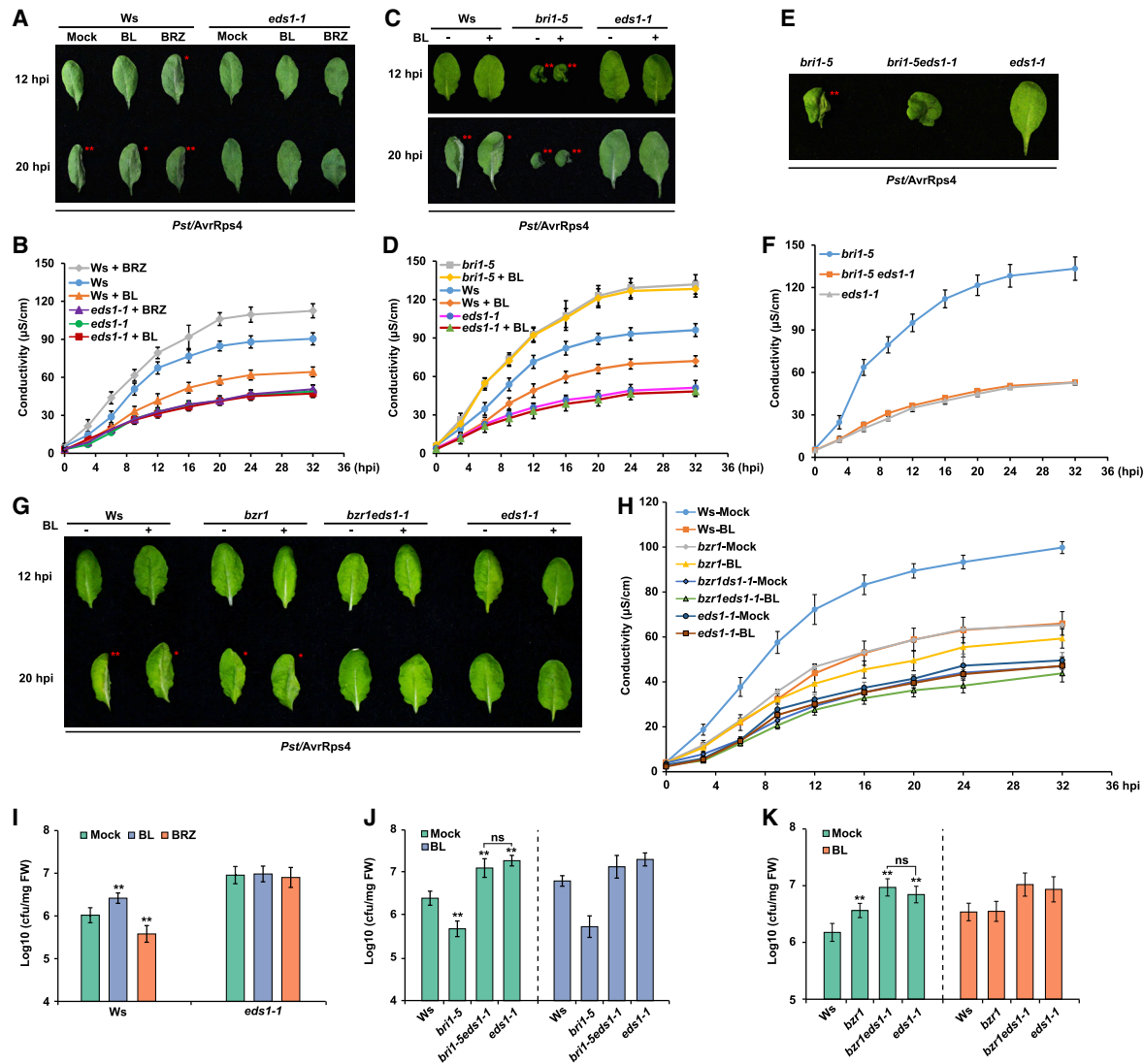


Figure 4. Attenuation of RPS4-controlled HR by activation of BR signaling or BZR1 mutation.

(A and B) Modulation of RPS4-controlled HR processes by exogenous application of brassinolide (BL) or brassinazole (BRZ). Four-week-old soil-grown Ws or *eds1-1* plants were pretreated with 1 μM BL or 2.5 μM BRZ for 3 or 10 h, followed by inoculation with the bacterial strain *Pst/AvrRps4* (OD_{600 nm} = 0.1). Foliar cell death was examined at 12 and 20 hpi, respectively **(A)**. For ion leakage measurement, leaf discs were prepared and vacuum infiltrated with *Pst/AvrRps4* (OD_{600 nm} = 0.05), followed by immersion in sterile water, and the conductivity was measured at the indicated time points **(B)**. *AvrRps4*-triggered HR response in Ws plants was attenuated by BL but enhanced by BRZ; it was abolished in *eds1-1* that lacked a functional EDS1.

(C and D) Enhancement of RPS4-controlled HR cell death **(C)** and ion leakage **(D)** in the BR-insensitive mutant *bri1-5*. Soil-grown Ws, *bri1-5*, and *eds1-1* plants were pretreated with 1 μM BL for 3 h, followed by inoculation with the bacterial strain *Pst/AvrRps4*. HR cell death and ion leakage were examined as described above. The enhancement was not seen in *eds1-1*.

(E and F) Abolishment of *AvrRps4*-triggered HR cell death and ion leakage in *bri1-5* in the absence of a functional EDS1. Soil-grown *bri1-5*, *bri1-5eds1-1* (double mutant), and *eds1-1* plants were used for *Pst/AvrRps4*-triggered HR cell death **(E)** and ion leakage analyses **(F)**. The cell death phenotypes **(E)** were recorded at 18 hpi, and ion leakage was determined at the indicated time points.

(G and H) Compromised HR cell death and ion leakage in the *bzo1* mutant after *Pst/AvrRps4* infection. Soil-grown Ws, *bzo1*, *bzo1eds1-1*, and *eds1-1* plants were treated with BL and inoculated with *Pst/AvrRps4* as above. Cell death was recorded at 12 and 20 hpi **(G)**, and ion leakage was measured at the indicated time points **(H)**. Values were means ± SD (*n* = 6).

(I–K) Elevated *Pst/AvrRps4* growth in plants treated with BL or in the *bzo1* mutant. Four-week-old plants of Ws, *eds1-1*, *bri1-5*, *bri1-5eds1-1*, *bzo1*, and *bzo1eds1-1* were treated with BL or BRZ (as indicated in each graph) for 3 or 10 h, followed by infiltration with *Pst/AvrRps4* (OD_{600 nm} = 0.0005) and quantification of bacterial titers at 3 dpi. CFU, colony-forming units. In **(A)**, **(C)**, **(E)**, and **(G)**, the single and double asterisks indicate mild and severe cell death, respectively. In **(I–K)**, error bars represent the SD of six measurements. ***P* < 0.01 (Student's *t*-test). The datasets shown are all typical of three independent experiments.

BZR1-EDS1 regulates plant growth and defense

Molecular Plant

overexpressing an NPR1-GFP fusion protein) (Mou et al., 2003) (Figure 3A). When treated with brassinolide (BL, a bioactive BR), hypocotyl elongation was promoted in all lines examined above, but compared with Col-0, the extent of the promotion was greater for *eds1-2*, *npr1-2*, *sid2*, and *NahG* plants than for *35S::EDS1-GFP* and *35S::NPR1-GFP* plants (Figure 3A).

In agreement with the above result, we observed that the higher the concentration of exogenously applied SA, the stronger the inhibition of hypocotyl elongation in both *Arabidopsis ecotype Wassilewskija* (Ws) and Col-0 plants (Figure 3B). However, the extent of the inhibition was attenuated in *eds1-2*, *bri1-5* (a BR-insensitive mutant caused by a mutation in the BR receptor BRI1, Noguchi et al., 1999), and *bak1-4* (a loss-of-function mutant of BAK1, which is the co-receptor of BRI1 in BR signaling, Li et al., 2002). BR signaling also stimulates petiole growth in *Arabidopsis* (Kim and Wang, 2010; Sun et al., 2010). Under mock conditions, petiole length was significantly longer in *eds1-2* than in Col-0 (Figure 3C and 3D). By contrast, the petiole length of *bak1-4* was much shorter than that of Col-0 (Figure 3C and 3D). Upon infection by the virulent pathogen *Pseudomonas syringae* pv. *tomato* (*Pst*) DC3000, which is known to upregulate EDS1 function and activate basal resistance (Feys et al., 2001), the petiole length of WT plants was significantly decreased, whereas no substantial reductions in petiole length were observed in *eds1-2* or *bak1-4* (Figure 3C and 3D).

The impairment of BR-promoted growth during *Pst* DC3000 infection or exogenous SA treatment was accompanied by the reduced expression of two representative BRRGs (*EXP8* and *SAUR15*) in WT Col-0, which was, however, alleviated in the *eds1-2* mutant (Figure 3E and 3F). This result was in line with decreased occupancy of BZR1 in the promoter regions of *EXP8* and *SAUR15* upon increasing EDS1 expression (Figure 2).

Activation of BR signaling suppresses RPS4-controlled ETI

To investigate the function of BZR1-EDS1 in TNL protein-mediated ETI, we analyzed the effect of BR signaling on RPS4-controlled HR cell death and its possible dependence on EDS1. RPS4, originally cloned from the *Arabidopsis ecotype* Ws and shown to form an immune receptor complex with RRS1, initiates HR cell death in response to the avirulent effector AvrRps4 from *P. syringae* pv. *lisi* (Hinsch and Staskawicz, 1996). We compared HR elicited by the bacterial strain *Pst* DC3000 carrying AvrRps4 (*Pst*/AvrRps4) in Ws and *eds1-1* (Parker et al., 1996), a dysfunctional mutant of EDS1 in the Ws background, in the presence of BL or brassinazole (BRZ, a potent BR biosynthesis inhibitor). In Ws plants, HR cell death and associated ion leakage were downregulated by BL but upregulated by BRZ relative to those in mock controls (Figure 4A and 4B). By contrast, HR cell death and ion leakage were abolished in *eds1-1* irrespective of BL or BRZ treatment (Figure 4A and 4B). Consistently, *Pst*/AvrRps4 growth was elevated in the BL-treated Ws plants but reduced in plants sprayed with BRZ, whereas no significant differences in pathogen growth were observed among the *eds1-1* plants treated with water, BL, or BRZ (Figure 4I). qRT-PCR analysis showed that the expression of *PR1*, a marker gene of defense activation (Fu and Dong, 2013), was induced by *Pst*/AvrRps4 challenge in Ws plants but

suppressed by exogenous BL application (supplemental Figure 5).

Compared with Ws plants that showed reduced HR cell death and ion leakage upon BL treatment, *bri1-5* plants exhibited substantially increased HR cell death and ion leakage, irrespective of BL application (Figure 4C and 4D). Furthermore, we generated a *bri1-5eds1-1* double mutant, and we compared HR cell death and ion leakage in *bri1-5eds1-1*, *bri1-5*, and *eds1-1*. The *bri1-5eds1-1* plants were developmentally and morphologically similar to *bri1-5* plants (supplemental Figure 6). But unlike *bri1-5*, *bri1-5eds1-1* did not show HR-associated cell death and ion leakage after challenge with *Pst*/AvrRps4 (Figure 4E and 4F). In fact, *bri1-5eds1-1* was indistinguishable from *eds1-1* in its lack of AvrRps4-triggered HR cell death and ion leakage phenotypes (Figure 4E and 4F). Consistently, growth of *Pst*/AvrRps4 was compromised in *bri1-5* but promoted in *bri1-5eds1-1* relative to the WT control, with *bri1-5eds1-1* and *eds1-1* exhibiting similar *Pst*/AvrRps4 growth (Figure 4J). Moreover, BL treatment had no significant effects on bacterial growth in the *bri1-5*, *bri1-5eds1-1*, and *eds1-1* mutants (Figure 4J). Together, these results indicate that activation of BR signaling by BL suppresses AvrRps4-triggered ETI and that EDS1 is epistatic to BRI1 in the regulation of RPS4-controlled ETI.

In contrast to the above result, BL treatment had no effect on the HR cell death and ion leakage phenotypes controlled by two CC-NB-LRR (CNL) R proteins, RPS2 or RPM1, in Col-0 plants: after challenged with the avirulent effector AvrRpt2 or AvrRpm1 (Boyes et al., 1998; Mackey et al., 2002, 2003), HR cell death and ion leakage were not significantly altered by BL application (supplemental Figure 7). This is consistent with the fact that EDS1 acts as an essential regulator of the ETI controlled by TNL proteins but not that controlled by CNLs.

BZR1 positively regulates RPS4-controlled ETI

To further study the function of the BZR1-EDS1 interaction in RPS4-controlled ETI, we generated a *bzr1* knockout mutant using CRISPR/Cas9 editing in both WT Ws and the *eds1-1* mutant. The *bzr1* mutation had a frameshifting nucleotide insertion in the *BZR1* coding sequence that eliminated BZR1 protein expression in both *bzr1* and *bzr1eds1-1* plants (supplemental Figure 8). We thus analyzed AvrRPS4-triggered ETI responses in *bzr1* and *bzr1eds1-1* with or without BL treatment. Compared with WT Ws, the *bzr1*, *bzr1eds1-1*, and *eds1-1* lines all showed compromised ETI responses, including decreased HR cell death and ion leakage and elevated *Pst*/AvrRps4 growth. These responses were more severely impaired in *bzr1eds1-1* and *eds1-1*, irrespective of BL treatment (Figure 4G, 4H, and 4K). These genetic and pathological analyses indicate that BZR1 positively regulates the RPS4-controlled ETI in an EDS1-dependent manner.

The cytoplasmic fraction of BZR1 is required for efficient development of RPS4-controlled ETI

The GSK3-like kinase BIN2 and its functional homoeologs play an important role in the cytoplasmic retention of BZR1 by phosphorylating BZR1 (Yan et al., 2009). LiCl and bikinin are potent inhibitors of GSK3-like kinases in *Arabidopsis*; their application leads to dephosphorylation and nuclear translocation of BZR1, thereby activating BR signaling (De Rybel et al., 2009; Kondo

Molecular Plant

et al., 2014). We therefore examined whether LiCl or bikinin treatment affected RPS4-controlled HR cell death. Compared with the control Ws plants not treated with LiCl or bikinin, those treated with either compound showed reduced ion leakage (supplemental Figure 9A). A similar decrease in ion leakage was observed in the *bri1-5* mutant treated with bikinin (supplemental Figure 9B). These observations point to the possibility that dephosphorylation and nuclear translocation of BZR1, caused by treatment with LiCl or bikinin, may underlie the suppression of RPS4-controlled ETI by BL application (Figure 4).

To analyze whether cytoplasmic retention and nuclear translocation of BZR1 have different effects on RPS4-mediated ETI, we generated *pBZR1::bzi1-1D-GFP* transgenic lines in the Ws background. The *bzi1-1D* mutation increases BZR1 accumulation in both the cytoplasm and nucleus but does not alter BZR1's subcellular distribution pattern (Gampala et al., 2007). In the mx3 transgenic line (*pBZR1::bzi1-1D-CFP* in the Col-0 background), expression of *bzi1-1D-CFP* decreases *Arabidopsis* stature and causes the development of darker green, smaller, and curved rosette leaves (Zhang et al., 2013). As expected, our *pBZR1::bzi1-1D-GFP* transgenic lines (no. 3 and no. 5) resembled mx3 in plant phenotypes (supplemental Figure 10). When inoculated with *Pst/AvrRps4*, the two independent *pBZR1::bzi1-1D-GFP* lines both showed substantially stronger HR cell death and ion leakage than Ws plants (Figure 5A and 5B; supplemental Figure 11). BL treatment suppressed the RPS4-controlled ETI in this set of experiments, but even so, the HR cell death and ion leakage phenotypes exhibited by BL-treated *pBZR1::bzi1-1D-GFP* lines were still more severe than those displayed by the Ws control without BL treatment (Figure 5A and 5B; supplemental Figure 11). Notably, the transcript level of *BZR1* was significantly upregulated in the Ws plants inoculated with *Pst/AvrRps4* relative to mock controls (Figure 5C). The protein level of *bzi1-1D-GFP* in *pBZR1::bzi1-1D-GFP* plants was substantially enhanced by *Pst/AvrRps4* but not by *Pst* DC3000 that did not express *AvrRps4* (Figure 5D).

Subsequently, we created a new type of transgenic line in the Ws background, *pBZR1::bzi1-1DΔNLS-GFP* (no. 2 and no. 4), in which the nuclear localization signal (NLS) sequence (18 residues) in *bzi1-1D* was deleted. The *bzi1-1DΔNLS* mutant protein had a reduced molecular mass (~34 kDa) compared with *bzi1-1D* (~37 kDa), and its distribution was restricted to the cytoplasm with or without BL treatment (Figure 5E and 5F). Remarkably, the *pBZR1::bzi1-1DΔNLS-GFP* plants grew and developed as WT Ws individuals (supplemental Figure 10), indicating that cytoplasmic retention and accumulation of *bzi1-1DΔNLS* ameliorates the growth inhibition associated with the *bzi1-1D* mutation (Zhang et al., 2013). After inoculation with *Pst/AvrRps4*, the *pBZR1::bzi1-1DΔNLS-GFP* plants showed enhanced HR cell death and ion leakage relative to Ws controls; these phenotypes were similar to those displayed by the *pBZR1::bzi1-1D-GFP* plants challenged with *Pst/AvrRps4* (Figure 5G and 5H). Consistently, growth of *Pst/AvrRps4* was attenuated in both *pBZR1::bzi1-1D-GFP* and *pBZR1::bzi1-1DΔNLS-GFP* plants compared with WT controls (Figure 5I). These results, together with the foregoing data, suggest that the cytoplasmic fraction of BZR1 is essential for efficient

BZR1-EDS1 regulates plant growth and defense

activation of RPS4-controlled ETI, whereas nuclear translocation of BZR1 is likely to be responsible for the suppression of RPS4-conditioned ETI following the activation of BR signaling by BL application or treatment with LiCl or bikinin (Figure 4A–4D and supplemental Figure 9).

Cytoplasmic BZR1 facilitates AvrRps4-triggered dissociation of EDS1 and RPS4

The above data prompted us to investigate how cytosolic BZR1 might regulate RPS4-controlled ETI. Because EDS1 is essential for RPS4-controlled ETI (see the Introduction), we first checked whether BZR1's interaction with EDS1 affected the stability of EDS1. We found that EDS1 protein accumulation was not altered by knocking out BZR1 (in *bzi1* plants), and BZR1 expression level was not affected in *eds1-1* plants (supplemental Figure 12). We then analyzed whether BZR1 protein level changed in response to *Pst/AvrRps4* inoculation in Ws plants using immunoblotting with a BZR1-specific antibody (Chen et al., 2019b). We found that *Pst/AvrRps4* infection decreased the amount of unphosphorylated BZR1 but increased the amount of phosphorylated BZR1, and this was especially evident when the cytoplasmic and nuclear fractions were analyzed (Figure 6A).

A crucial step in RPS4-controlled ETI is the dissociation of EDS1 and RPS4 by binding of *AvrRps4* to EDS1 in the cytoplasm (Bhattacharjee et al., 2011; Heidrich et al., 2011). Motivated by this knowledge and the finding that BZR1 interacted with EDS1, we hypothesized that BZR1 may promote *AvrRps4*-triggered dissociation of EDS1 and RPS4 in the cytoplasm. To test this idea, we expressed *bzi1-1D-GFP* or GFP in protoplasts of *RPS4-HA/rps4-2*, a complementation line of *rps4-2* that expresses HA-tagged RPS4 under its native promoter (Pike et al., 2019). We then investigated the effects of BZR1 on the dissociation of EDS1 and RPS4-HA. With the expression of *bzi1-1D-GFP*, the amount of EDS1 co-precipitated with RPS4-HA was markedly decreased compared with that of GFP (Figure 6B and supplemental Figure 13).

We then analyzed in more detail the effect of cytoplasmic BZR1 on *AvrRps4*-triggered dissociation of EDS1 and RPS4 in *RPS4-HA/rps4-2* plants. For this purpose, we used both WT *AvrRps4* and a nonfunctional mutant of *AvrRps4*, *AvrRps4* KR^YAAAA (Saucet et al., 2015), as well as BL treatment to artificially alter the accumulation of BZR1 in the cytoplasm. The cytoplasmic fractions from various plant samples were isolated and subjected to Co-IP analysis. As anticipated, the bacterial strain carrying *AvrRps4* KR^YAAAA (designated *Pst/mAvrRps4*) failed to trigger HR (supplemental Figure 14). BL treatment of uninfected plants drastically decreased cytoplasmic BZR1 accumulation but enhanced the EDS1 co-precipitated with RPS4-HA (Figure 6C, lane 4 versus lane 1), indicating that lowering cytoplasmic BZR1 enhanced the EDS1-RPS4 interaction. In the absence of BL treatment, inoculation with *Pst/AvrRps4* increased cytoplasmic BZR1 but markedly decreased the amount of EDS1 co-precipitated with RPS4-HA (Figure 6C, lane 2 versus lane 1), suggesting that the increased cytoplasmic BZR1 facilitated *AvrRps4*-triggered dissociation of EDS1 from RPS4. With BL treatment, infection by *Pst/AvrRps4* also increased cytoplasmic BZR1, albeit to a lesser extent

BZR1-EDS1 regulates plant growth and defense

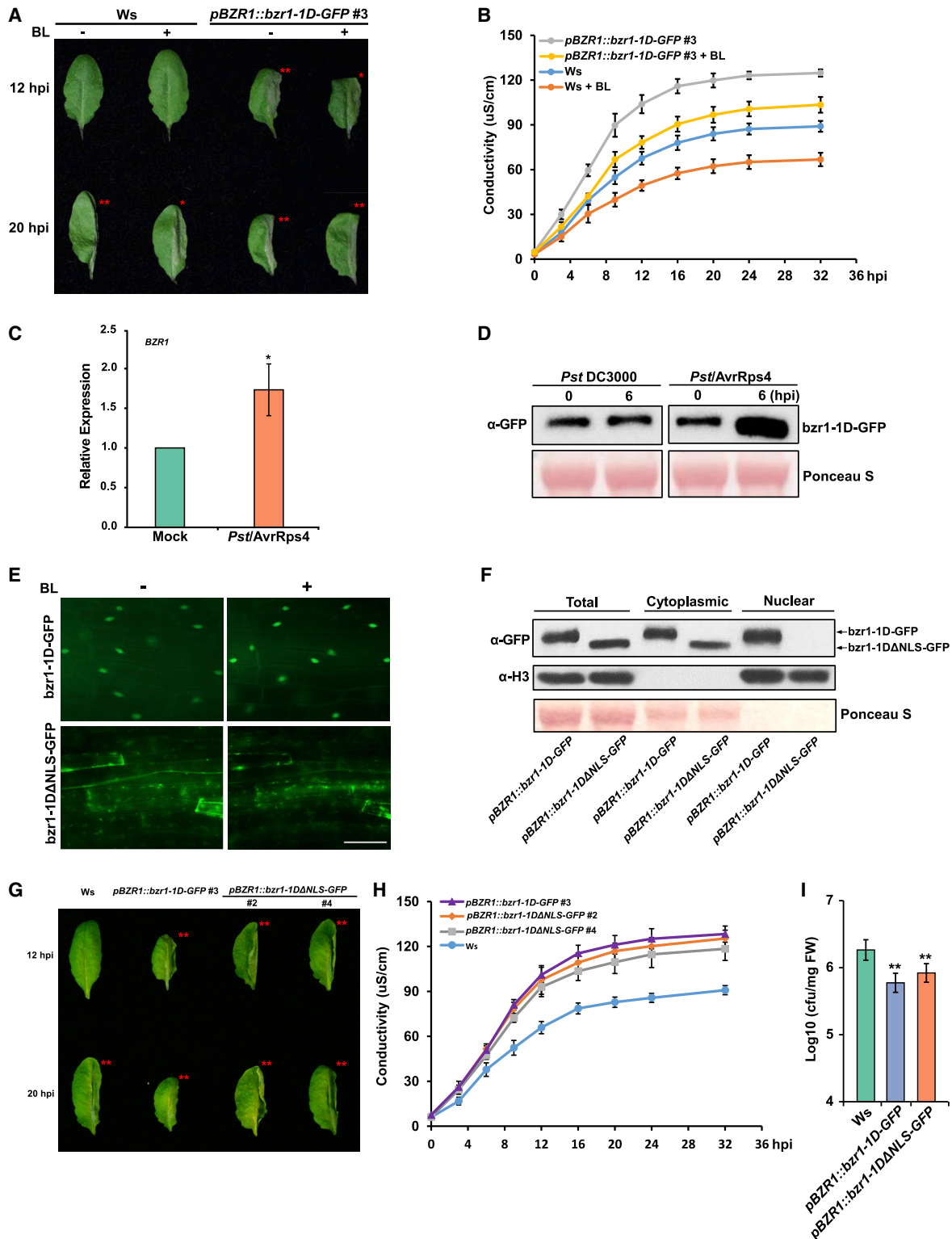


Figure 5. Requirement of cytoplasmic fraction of BZR1 for efficient activation of RPS4-controlled HR.

(A and B) Enhancement of *Pst/AvrRps4*-triggered HR cell death and ion leakage in *pBZR1::bzt1-1D-GFP* transgenic plants. Soil-grown Ws and *pBZR1::bzt1-1D-GFP* no. 3 transgenic plants were pretreated with 1 μ M BL for 3 h, followed by inoculation with *Pst/AvrRps4*. Cell death was recorded at 12 and 20 hpi (A), and ion leakage was measured at the indicated time points (B). (C) Upregulation of *BZR1* expression by infection with *Pst/AvrRps4*. qRT-PCR analysis was performed in Ws plants inoculated with *Pst/AvrRps4* ($OD_{600\text{ nm}} = 0.05$) for 6 h. Amplification of *UBQ5* was used as an internal control. Error bars represent the SD of three independent experiments. * $P < 0.05$ (Student's *t*-test).

(legend continued on next page)

Molecular Plant

(Figure 6C, lane 5 versus lane 1), but the amount of EDS1 co-precipitated with RPS4-HA was substantially enhanced compared with that without BL treatment (Figure 6C, lane 5 versus lane 2), thereby confirming that an increase in cytoplasmic BZR1 promoted AvrRps4-triggered dissociation of EDS1 and RPS4. By contrast, infection of *RPS4-HA/rps4-2* plants by *Pst/mAvrRps4* did not obviously affect the interaction between EDS1 and RPS4, with or without BL treatment, as demonstrated by the substantial amount of EDS1 co-precipitated with RPS4-HA (Figure 6C, lanes 3 and 6). Collectively, the above biochemical data support the notion that cytoplasmic BZR1 is required for efficient development of RPS4-conditioned ETI by facilitating AvrRps4-triggered dissociation of EDS1 and RPS4.

DISCUSSION

Functions of the BZR1-EDS1 module and underlying molecular mechanism

In this work, we identified and analyzed a previously unreported interaction module composed of BZR1 and EDS1, and we revealed the functions of this module in the regulation of plant growth and defense in both basal resistance and TNL receptor-controlled ETI (Figure 7).

In the basal resistance induced in a compatible pathosystem, upregulation of EDS1 expression suppresses BR-promoted growth processes, e.g., hypocotyl and petiole elongation. This suppression is associated with inhibition of BZR1's transcriptional activities and decreased expression of growth-related BRRGs (e.g., *EXP8* and *SAUR15*), which is caused by reduced occupancy of BZR1 in the promoter region of its target genes owing to EDS1 binding to BZR1 (Figure 7). Because it is well known that virulent pathogen infection upregulates EDS1 expression and that a positive feedback loop exists between EDS1 accumulation and SA content (Feys et al., 2001), it is understandable that perturbing SA level or perception alters the function of the BZR1-EDS1 module in growth-defense coordination in basal resistance.

In RPS4-controlled ETI, RPS4 is present in both the cytoplasm and the nucleus, with perception of AvrRps4 by the RPS4/RRS1 receptor complex occurring in the nucleus (Wirthmueller, et al., 2007). Furthermore, AvrRps4-triggered dissociation of EDS1 and RPS4 in the cytoplasm has been found to be essential for full activation of RPS4-controlled ETI (Bhattacharjee et al., 2011; Heidrich et al., 2011). Based on the results of this work, we suggest that the cytoplasmic pool of BZR1, which was

BZR1-EDS1 regulates plant growth and defense

increased substantially by an avirulent effector (i.e., AvrRps4, Figure 6A), enables efficient development of HR by facilitating the AvrRps4-triggered dissociation of EDS1 and RPS4 in the cytoplasm (Figure 7). Maintenance of an appropriate amount of cytoplasmic BZR1 is crucial for keeping RPS4-mediated ETI at a proper level, as HR was attenuated by decreasing BZR1's cytoplasmic retention (by exogenous application of BL, LiCl, or bikinin) or aggravated by increasing BZR1's cytoplasmic accumulation (by BRZ application or the *bzr1-1D* and *bzr1-1DΔNLS* mutations).

Clearly, in both types of immunity, pathogen defense is activated with concomitant inhibition of plant cell growth. A functional EDS1 is required for both defense activation and growth inhibition. In basal resistance, growth inhibition is mediated, at least in part, by downregulation of BZR1's transcriptional activities due to binding of EDS1 to BZR1 in the nucleus. In TNL protein-controlled ETI, growth inhibition (indicated by localized cell death) involves increased accumulation of cytoplasmic BZR1, binding of cytoplasmic BZR1 to EDS1, and promotion of HR-associated defense processes by the BZR1-EDS1 interaction in the cytoplasm. We noted that knocking out *BZR1* or over-accumulation of *bzr1-1D* did not substantially affect *Pst* DC3000 proliferation (supplemental Figure 15), indicating that *BZR1* alone may not play a significant role in basal resistance.

Although PAD4 and SAG101 are required for the regulation of plant immunities by EDS1 (Cui et al., 2015; Feys et al., 2005), we found here that BZR1 interacted with EDS1 but not with PAD4 and SAG101 (supplemental Figure 1A). Furthermore, we observed that PAD4 and SAG101 were not essential for EDS1 to impede binding of BZR1 to the promoter *cis*-elements of two BRRGs (Figure 3A and 3B). Thus it is possible that PAD4 and SAG101 may not be involved in the regulation of plant growth and defense by the BZR1-EDS1 module. Interestingly, we observed that cytoplasmic BZR1 could also promote the dissociation of EDS1 and RPS4 when tested in *Nicotiana benthamiana* using transiently expressed proteins (supplemental Figure 16). Considering that *Arabidopsis* and *N. benthamiana* differ substantially in the expression and function of homoeologous PAD4 and SAG101 proteins (Gantner et al., 2019), this provides further evidence for the possibility discussed above. Nevertheless, more work is needed to verify this possibility.

Compared with previous studies that show the inhibition of PTI by BZR1 and HBI1 (Lozano-Duran et al., 2013; Fan et al., 2014; Malinovsky et al., 2014), our work is unique in demonstrating that

(D) Elevation of *bzr1-1D*-GFP accumulation by *Pst/AvrRps4* infection of *pBZR1::bzr1-1D-GFP* transgenic plants. An anti-GFP antibody was used to detect *bzr1-1D*-GFP by immunoblotting. The increased *bzr1-1D*-GFP accumulation may occur both transcriptionally and post-transcriptionally, as the BZR1 promoter responded positively to *Pst/AvrRps4* infection (**C**), and *bzr1-1D* could resist ubiquitin-mediated degradation.

(E and F) Abolishment of nuclear localization of *bzr1-1D* protein by deletion of its nuclear localization signal (NLS). Transgenic *Arabidopsis* plants expressing *bzr1-1D*-GFP or *bzr1-1DΔNLS*-GFP (lacking the NLS) were grown on $\frac{1}{2}$ MS medium for 3 days, then treated with 1 μ M BL for 3 h. Nuclear accumulation was observed for *bzr1-1D*-GFP but not *bzr1-1DΔNLS*-GFP, irrespective of BL treatment (**E**). Immunoblotting using anti-GFP antibody confirmed the accumulation of *bzr1-1D*-GFP, but not *bzr1-1DΔNLS*-GFP, in the nuclear fraction (**F**). Immunodetection of histone H3 was used to verify the purity of the different cellular fractions. Scale bar, 10 μ m.

(G and H) Increase in *Pst/AvrRps4*-triggered HR cell death (**G**) and ion leakage (**H**) in the *pBZR1::bzr1-1DΔNLS-GFP no. 2* and *no. 4* transgenic plants relative to WT Ws controls. *pBZR1::bzr1-1DΔNLS-GFP* resembled *pBZR1::bzr1-1D-GFP* in HR-associated cell death and ion leakage. The cell death and ion leakage phenotypes were recorded as described above.

(I) Attenuated *Pst/AvrRps4* growth in *pBZR1::bzr1-1D-GFP* and *pBZR1::bzr1-1DΔNLS-GFP* transgenic lines. Four-week-old soil-grown plants were infiltrated with *Pst/AvrRps4* ($OD_{600\text{ nm}} = 0.0005$), and pathogen growth was quantified at 3 dpi. CFU, colony-forming units. In (**A**) and (**G**), the single and double asterisks indicate mild and severe cell death, respectively. In (**B**), (**H**), and (**I**), error bars represent the SD of six measurements. * $P < 0.05$, ** $P < 0.01$ (Student's *t*-test). The experiments shown above were repeated at least three times with similar results.

BZR1-EDS1 regulates plant growth and defense

Molecular Plant

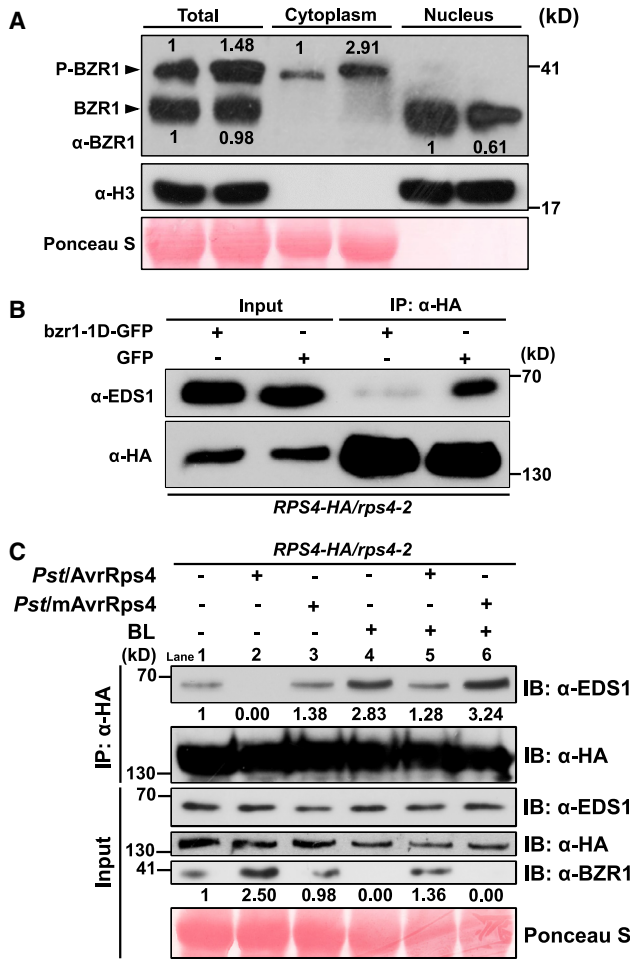


Figure 6. Promotion of AvrRps4-triggered dissociation of EDS1 and RPS4 by cytoplasmically located BZR1.

(A) Upregulation of BZR1 accumulation in the cytoplasm by *Pst/AvrRps4* infection. Total, cytoplasmic, and nuclear protein fractions, prepared from leaf tissues of 4-week-old WT Ws plants infiltrated with mock solution or *Pst/AvrRps4* ($OD_{600\text{ nm}} = 0.2$) for 6 h, were subjected to immunoblotting using an anti-BZR1 antibody. Relative band intensities were obtained using ImageJ software, and the value of the control sample was set to 1 to facilitate comparison.

(B) Promotion of the dissociation of EDS1 and RPS4-HA by *bzr1-1D-GFP*. Protoplasts of *RPS4-HA/rps4-2* were transfected with *pBZR1::bzr1-1D-GFP* or *p35S::GFP*, IP was conducted using Anti-HA Magnetic Beads, and immunoblotting was performed using anti-EDS1 or anti-HA antibodies.

(C) AvrRps4-triggered dissociation of EDS1 and RPS4-HA is promoted by cytoplasmic BZR1. Leaves of *RPS4-HA/rps4-2* plants were treated with 1 μM BL or mock solution for 3 h and inoculated with *Pst/AvrRps4* or *Pst/mAvrRps4* (*Pst* DC3000 carrying AvrRps4 KRVY^{AAA}) as above. Then cytoplasmic fractions prepared from control and treated samples were used for coIP assays. IP was conducted with Anti-HA Magnetic Beads, and immunoblotting (IB) was performed using anti-BZR1, anti-EDS1, or anti-HA antibodies. Relative band intensities were obtained using ImageJ software, and the value of the control sample (lane 1) was set to 1 to facilitate comparison. The data depicted in **(A–C)** were reproducible in three separate experiments.

activation of defense suppresses BR-promoted growth in both basal resistance and TNL protein-conditioned ETI via the BZR1-EDS1 interaction. Consistent with our work, the onset of flg22-induced basal defense leads to downregulated expression of key

BR biosynthesis genes (Jimenez-Gongora et al., 2015). Similar to our work, a previous study uncovered a novel interaction module, DELLA-EDS1, that functions in plant growth-defense trade-offs in *Arabidopsis* (Li et al., 2019). Discovery of DELLA-EDS1 and BZR1-EDS1 modules in previous and current studies suggests that EDS1 may be a common interaction target for important phytohormone signaling components during the regulation of plant growth and defense response by different hormones.

BZR1 has multiple homoeologs (e.g., BES1), and they function similarly in BR-promoted growth. Therefore, it will be interesting to examine whether BES1 also binds to EDS1 in further research. It will also be interesting to test whether HBI1 interacts with EDS1, as HBI1 has been shown to regulate the trade-offs between plant growth and immunity (Fan et al., 2014; Malinovsky et al., 2014). However, based on the findings that BZR1 expression was not markedly downregulated by virulent pathogen infection and exogenous SA (supplemental Figure 17) and that BZR1 expression and protein accumulation were both considerably increased by *Pst/AvrRps4* inoculation (Figure 5C and 5D), BZR1 may be a major interactor of EDS1 in the regulation of plant growth and immunity. Other BR signaling components, if they do interact with EDS1, may help to fine-tune such regulation in different plant species and organs, at different developmental stages, in different environments, and/or against different pathogens.

A new function identified for the cytoplasmic fraction of BZR1

Based on current understanding, the nuclear pool of BZR1 plays important roles in regulating BRRG expression and participating in crosstalk with other signaling pathways, whereas the cytoplasmic fraction of BZR1 acts as a reservoir for nuclear BZR1 (Kim and Wang, 2010). No other functions have been assigned to cytoplasmic BZR1 to date. Here, we reveal that cytoplasm-located BZR1 is needed for the efficient development of RPS4-controlled ETI, thus identifying a previously unknown function for the cytoplasmic fraction of BZR1.

Remarkably, we found that transgenically expressed *bzr1-1D Δ NLS* not only enhanced AvrRps4-triggered HR but also mitigated the growth retardation phenotype of *bzr1-1D*. This raises the possibility that *bzr1-1D Δ NLS* may be useful for lessening the suppression of BR-promoted growth by EDS1-mediated pathogen defense. Although breaking the trade-off between growth and immunity may be harmful to plant fitness and long-term survival in natural environments, better coordination between growth and defense may allow simultaneous improvement of growth performance and disease resistance, and hence yield level, of crop plants under artificial cultivation conditions. Therefore, the potential value of *bzr1-1D Δ NLS* for optimizing growth and defense balance in crop plants merits further investigation.

Potential of the BZR1-EDS1 module in agricultural application

The identification and analysis of the BZR1-EDS1 module in *Arabidopsis* raise the question whether analogous modules exist and function in other plant and crop species. In a preliminary test with the monocotyledonous crop plant common wheat (*Triticum aestivum*, AABBDD, $2n = 6x = 42$), a hexaploid with three homeologs

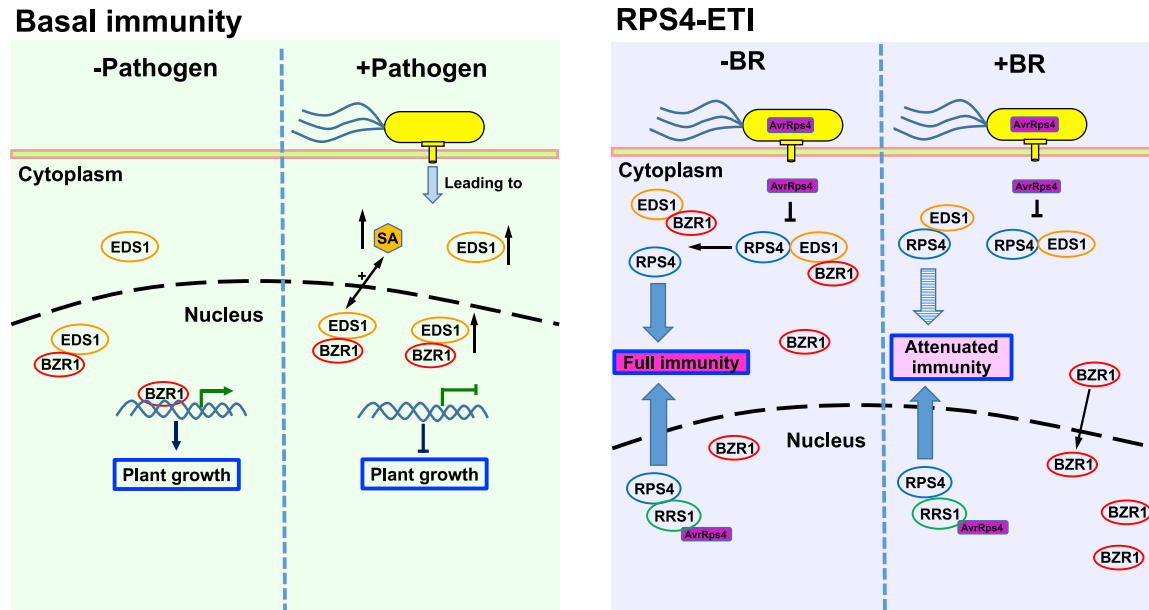


Figure 7. A working model for the regulation of plant growth and pathogen defense by the BZR1-EDS1 module.

When basal immunity is activated in a compatible pathosystem, EDS1 expression and function are upregulated, leading to increased accumulation of SA, which further enhances EDS1 expression in a positive feedback loop. The upregulated EDS1 interacts with BZR1 and inhibits its transcriptional activities, thus decreasing the expression of BR-responsive genes (e.g., *EXP8* and *SAUR15*) and BR-promoted plant growth. In RPS4-controlled ETI, AvrRps4 triggers the dissociation of EDS1 and RPS4 in the cytoplasm and is sensed by the RPS4/RRS1 complex in the nucleus; both of these events are required to fully activate the immunity. The cytoplasmic pool of BZR1 enables the efficient development of robust immunity (HR) by facilitating the dissociation of EDS1 and RPS4. Enhancement of BR signaling (e.g., by brassinolide treatment) attenuates RPS4-controlled immunity by increasing BZR1's nuclear translocation.

of most genes (International Wheat Genome Sequencing Consortium et al., 2018), protein–protein interactions were observed between TaBZR1 homeologs and those of TaEDS1 in Y2H assays (supplemental Figure 18). Thus, the BZR1-EDS1 interaction module is probably conserved in both dicot (e.g., *Arabidopsis*) and monocot (common wheat) plants.

Following the points discussed above, we hypothesize that transgenically expressed *bzr1-1DΔNLS* protein may be employed as a surrogate for endogenous BZR1 to serve as the interacting partner of EDS1 for expediting pathogen defense. This may diminish the inhibitory binding of EDS1 to endogenous BZR1, thus enabling defense activation without sacrificing BR signaling and BR-promoted plant growth and eventually leading to concurrent improvements of both growth and immunity in crop plants with higher productivity.

METHODS

Plant materials, growth conditions, and oligonucleotide primers and probes

Arabidopsis thaliana plants were grown in a greenhouse or a growth chamber under a 12 h light/12 h dark cycle and 75% humidity at 20°C–23°C. The *Arabidopsis* lines used for *Pst*/AvrRps4-triggered HR cell death and ion leakage analyses were generated in the *Ws* ecotype background, including *eds1-1*, *bri1-5*, *pBZR1::bzr1-1D-GFP*, *pBZR1::bzr1-1DΔNLS-GFP*, and the *bzr1* knockout mutants developed using CRISPR/Cas9-mediated editing (see below). The *RPS4-HA/rps4-2* transgenic line reported by Pike et al. (2019) was used to analyze the effect of cytoplasmic BZR1 on RPS4-controlled ETI. The oligonucleotide primers and probes used in this work are listed in supplemental Table 1.

Plasmid construction

Coding regions of *BZR1* and *EDS1* without a stop codon were cloned into the pDONR207 vector by BP reaction (Invitrogen, USA). To generate C-terminal GFP-tagged proteins, *BZR1* was cloned into the modified pMDC83 vector by LR reaction (Chen et al., 2019a). To generate *pBZR1::bzr1-1D-GFP*, the *bzr1-1D* sequence, including the promoter and coding region without the stop codon, was isolated from genomic DNA of the *bzr1-1D* mutant, followed by cloning into pDONR207 and then into the pMDC107 vector. To delete the NLS of the *bzr1-1D* protein sequence, site-directed mutagenesis was carried out on the *pBZR1::bzr1-1D* entry construct (amino acids 22–39 of BZR1) using the QuikChange Site-Directed Mutagenesis kit (Agilent, USA). The resulting construct was cloned into pMDC107. To generate vectors for the transient gene expression assays, the *BZR1* or *EDS1* coding region was ligated into the GUS-removed pBI221 vector between the 35S promoter and the NOS terminator to create the effector constructs. The promoter fragment of *EXP8* (1969 bp) or *SAUR15* (1323 bp) was ligated upstream of the GUS reporter in pBI221 after removing the 35S promoter to create the reporter constructs. All constructs were verified by sequencing.

qRT-PCR assays

Total RNA isolation and first-strand cDNA synthesis were performed as described previously (Chen et al., 2019a). qRT-PCR assays were conducted on a 7300 Real-time PCR System (Applied Biosystems, USA) using SYBR Green SuperMix (Quanta Biosciences, USA). *UBIQUITIN5 (UBQ5)* (*At3g62250*) was used as an internal control.

Y2H analysis

Yeast strain AH109 was co-transformed with pGBKT7-BZR1/TaBZR1 and the pGADT7 vector control or pGADT7-EDS1/TaEDS1/PAD4/SAG101 according to the Clontech yeast transformation protocol, and yeast colonies were selected on synthetic dextrose (SD)-Trp-Leu (DD) plates. Fresh

BZR1-EDS1 regulates plant growth and defense

Molecular Plant

single colonies were grown in SD/-Leu/-Trp liquid medium overnight at 30°C. The yeast cultures were diluted to $OD_{600\text{ nm}} = 1, 0.1, \text{ or } 0.01$ with sterilized 0.9% (w/v) NaCl solution. Then 10 μl of the diluted suspensions was spotted on SD/-Leu/-Trp and SD/-Leu/-Trp/-His plates with or without 3-amino-1,2,4-triazole (3-AT, 50 mM for pGBKT7-BZR1/TaBZR1). Yeast growth on the two types of plate was observed after 4–7 days at 30°C.

In vitro pull-down experiment

In vitro pull-down assays were performed as described previously (Chen et al., 2019a). Recombinant GST-fused EDS1 was purified using glutathione beads (GE Healthcare, USA). The 6 \times His-MBP-BZR1 recombinant protein was purified using Ni-NTA agarose (QIAGEN, Germany). The GST or GST-EDS1 proteins (5 μg each) immobilized on MagneGST Glutathione beads were combined with 1 mg of purified 6 \times His-MBP-BZR1 in 1 ml of binding buffer and incubated overnight at 4°C. The beads were then washed five times with a washing buffer. Proteins were eluted and separated on SDS-PAGE gels, and protein blots were probed using anti-6 \times His or anti-GST antibodies (Invitrogen, USA).

Co-IP assays

Co-IP assays were performed as described previously (Chen et al., 2019a). In brief, *Arabidopsis* leaves expressing different constructs as indicated were homogenized with protein extraction buffer and centrifuged at 20 000 g for 20 min at 4°C twice. GFP or GFP-tagged proteins were immunoprecipitated with GFP-Trap Magnetic Agarose beads (ChromoTek, Germany), and HA-tagged proteins were immunoprecipitated with Anti-HA Magnetic Beads (Thermo, USA). For protein blots, GFP, Flag, and HA fusion proteins were probed with anti-GFP (NEB, USA), anti-Flag (Sigma, USA), and anti-HA (3F10) (Roche, USA) antibodies, respectively. EDS1 or BZR1 was probed with an anti-EDS1 (Agriser, Sweden) or an anti-BZR1 (Youke Biotechnology, Shanghai, China) antibody.

BiFC

The coding sequence of BZR1 or EDS1 was introduced into the pUC-SPYCE or pUC-SPYNE vector (Walter et al., 2004). EDS1-YFP^N was co-transformed with BZR1-YFP^C or the empty vector into *Arabidopsis* mesophyll protoplasts, which were isolated and transfected following a previous method (Sheen, 2001). At least 200 transfected protoplasts were examined for BiFC signals using an Olympus FLUOVIEW FV1000 confocal microscope (Olympus, Tokyo, Japan).

Transient gene expression

Arabidopsis transient expression assays were performed as described previously (Tang et al., 2015). The BZR1 and EDS1 effector constructs and the GUS reporters driven by the *EXP8* or *SAUR15* promoter (see above) were appropriately combined and introduced into *Arabidopsis* mesophyll protoplasts. A *p35S:LUC* vector (Sato et al., 2014) was used as an internal control. The transfected protoplasts were cultured for 12 h in darkness. 4-Methylumbelliferone fluorescence and LUC luminescence were measured using a luminometer (Promega, USA). Relative GUS activity was determined by normalizing against the luciferase activity.

EMSA

GST, GST-EDS1, GST-PAD4, GST-SAG101, 6 \times His-MBP, or 6 \times His-MBP-BZR1 were each expressed and purified from *Escherichia coli* strain C41. Biotin-labeled synthetic oligonucleotides (Invitrogen, USA) were annealed with unlabeled oligonucleotides and then used as probes. DNA-protein binding reaction and detection were accomplished using a LightShift Chemiluminescent EMSA Kit (Thermo Fisher Scientific, USA). In brief, the labeled DNA probes were incubated for 30 min with 100 ng of 6 \times His-MBP-BZR1 protein with or without GST-EDS1 or the GST control in the binding buffer. The resulting products were then subjected to native polyacrylamide gel electrophoresis, followed by transfer to a nylon mem-

brane, which was used for detection of EMSA signals according to the manufacturer's instructions. To test whether PAD4 and SAG101 were involved in the interference of BZR1's *cis*-element binding activity by EDS1, a similar set of EMSAs was performed with GST-PAD4 and GST-SAG101 included (supplemental Figure 3A and 3B).

ChIP-qPCR

ChIP-qPCR assays were performed as described previously (Bowler et al., 2004). WT Col-0 and two different *Arabidopsis* lines, *pBZR1::bzt1-1D-CFP/eds1-2* and *pBZR1::bzt1-1D-CFP/Col-0*, were used. The 14-day-old seedlings were treated with SA for 24 h. Nuclei and chromatin were isolated from each sample (3 g). The chromatin was sonicated and then immunoprecipitated with GFP-Trap beads or control empty beads at 4°C overnight. The immunoprecipitated DNA was recovered and analyzed in triplicate by real-time qPCR with gene-specific primers. Fold enrichment was calculated by comparison with the internal control performed by amplifying the *ACTIN2* gene. All primers are listed in supplemental Table 1.

Cell death, ion leakage analysis, and quantification of bacterial growth

HR cell death was photographed at the desired time points. For ion leakage measurement, leaf disks were vacuum infiltrated with the desired bacterial strain, *Pst/AvrRpS4* ($OD_{600\text{ nm}} = 0.05$ for plants of the Ws ecotype background) or *Pst/AvrRpt2* (*Pst/AvrRpm1*) ($OD_{600\text{ nm}} = 0.05$ for Col-0 plants), then washed in distilled water for 30 min. Subsequently, eight leaf discs per replicate were transferred to a 50-ml sterile conical tube containing 8 ml distilled water. The conductivity was determined at different time points using an Orion Star A222 Conductivity Portable Meter (Thermo Fisher Scientific, USA). Measurement of bacterial growth was accomplished as described by Chen et al. (2019a).

Generation of *bzt1* mutants using CRISPR/Cas9-mediated editing

The CRISPR/Cas9 vector pHEC-401 developed by Wang et al. (2015) was used to generate *bzt1* mutants in WT Ws and *eds1-1* backgrounds with the guide RNA sequence GAGAAAGGGAGAATAATCGG. Preparation of genome-editing constructs and *Agrobacterium*-mediated transformation were accomplished as described previously (Wang et al., 2015). T1 transgenic plants were selected on MS medium containing 25 mg l^{-1} hygromycin. The guide RNA target site was PCR amplified and sequenced to determine the mutations introduced into the BZR1 coding region. The primer sets used are listed in supplemental Table 1.

Preparation of nuclear and cytoplasmic fractions

Cytoplasmic and nuclear fractions were prepared as described previously (Wang et al., 2011). In brief, 3-week-old *Arabidopsis* or tobacco leaves expressing the desired proteins were homogenized with lysis buffer. The homogenates were filtered through two layers of miracloth. The flow-through was centrifuged at 1500 g for 10 min at 4°C. Then the supernatant was centrifuged at 10 000 g for 10 min at 4°C and collected as the cytosolic fraction. The nuclear pellet was rinsed and finally resuspended in the lysis buffer. The cytosolic and nuclear fractions thus obtained were analyzed by immunoblotting and/or coIP assays using appropriate antibodies. Histone 3 was used as a nuclear marker to verify the purities of the cytosolic and nuclear fractions.

SUPPLEMENTAL INFORMATION

Supplemental information can be found online at *Molecular Plant Online*.

FUNDING

This work was supported by grants from the National Natural Science Foundation of China (91935304), the Innovative Postdoctoral Research Initiative of Henan Province (to G.Q.), and the National Science Foundation (EAGER grant 1464527 and grant IOS-1758994 to Z.Q.F.).

Molecular Plant

AUTHOR CONTRIBUTIONS

G.Q., D.W.W., and Z.Q.F. conceived the project. G.Q. performed the majority of the experiments. D.W. assisted with the generation of *bzr1* mutants. H.Y.Z. conducted the Y2H assays involving TaBZR1 and TaEDS1. X.F.T. and Y.P.W. provided assistance in transient expression assays. Z.Z.G., J.Y.C., H.C., and J.C. helped with the ETI analysis. M.-Y.B. and F.Q.L. provided critical discussion. G.Q., Z.Q.F., and D.W.W. jointly wrote the manuscript.

ACKNOWLEDGMENTS

We thank Professor Walter Gassmann (University of Missouri) for providing the seeds of *RPS4-HA/rps4-2* and Mr. Vitali Sikirzhyski for help with confocal microscopy. The authors declare no competing interests.

Received: December 7, 2020

Revised: February 7, 2021

Accepted: August 12, 2021

Published: August 17, 2021

REFERENCES

- Bernardo-García, S., de Lucas, M., Martínez, C., Espinosa-Ruiz, A., Davière, J., and Prat, S.** (2014). BR-dependent phosphorylation modulates PIF4 transcriptional activity and shapes diurnal hypocotyl growth. *Genes Dev.* **28**:1681–1694.
- Bhattacharjee, S., Halane, M.K., Kim, S.H., and Gassmann, W.** (2011). Pathogen effectors target *Arabidopsis* EDS1 and alter its interactions with immune regulators. *Science* **334**:1405–1408.
- Bittel, P., and Robatzek, S.** (2007). Microbe-associated molecular patterns (MAMPs) probe plant immunity. *Curr. Opin. Plant Biol.* **10**:335–341.
- Bowler, C., Benvenuto, G., Laflamme, P., Molino, D., Probst, A.V., Tariq, M., and Paszkowski, J.** (2004). Chromatin techniques for plant cells. *Plant J.* **39**:776–789.
- Boyes, D.C., Nam, J., and Dangl, J.L.** (1998). The *Arabidopsis thaliana* RPM1 disease resistance gene product is a peripheral plasma membrane protein that is degraded coincident with the hypersensitive response. *Proc. Natl. Acad. Sci. U S A* **95**:15849–15854.
- Caplan, J., Padmanabhan, M., and Dinesh-Kumar, S.P.** (2008). Plant NB-LRR immune receptors: from recognition to transcriptional reprogramming. *Cell Host Microbe* **3**:126–135.
- Chang, M., Zhao, J.P., Chen, H., Li, G.Y., Chen, J., Li, M., Palmer, I.A., Song, J.Q., Alfano, J.R., Liu, F.Q., et al.** (2019). PBS3 protects EDS1 from proteasome-mediated degradation in plant immunity. *Mol. Plant* **12**:678–688.
- Chen, J., Mohan, R., Zhang, Y., Li, M., Chen, H., Palmer, I.A., Chang, M., Qi, G., Spoel, S.H., Mengiste, T., et al.** (2019a). NPR1 promotes its own and target gene expression in plant defense by recruiting CDK8. *Plant Physiol.* **181**:289–304.
- Chen, L., Gao, Z., Zhao, Z., Liu, X., Li, Y., Zhang, Y., Liu, X., Sun, Y., and Tang, W.** (2019b). BZR1 family transcription factors function redundantly and indispensably in BR signaling but exhibit BRI1-independent function in regulating anther development in *Arabidopsis*. *Mol. Plant* **12**:1408–1415.
- Cui, H., Gobbato, E., Kracher, B., Qiu, J., Bautor, J., and Parker, J.E.** (2017). A core function of EDS1 with PAD4 is to protect the salicylic acid defense sector in *Arabidopsis* immunity. *New Phytol.* **213**:1802–1817.
- Cui, H., Tsuda, K., and Parker, J.E.** (2015). Effector-triggered immunity: from pathogen perception to robust defense. *Annu. Rev. Plant Biol.* **66**:487–511.
- De Bruyne, L., Höfte, M., and De Vleeschauwer, D.** (2014). Connecting growth and defense: the emerging roles of brassinosteroids and gibberellins in plant innate immunity. *Mol. Plant* **7**:943–959.
- De Rybel, B., Audenaert, D., Vert, G., Rozhon, W., Mayerhofer, J., Peelman, F., Coutuer, S., Denayer, T., Jansen, L., Nguyen, L., et al.** (2009). Chemical inhibition of a subset of *Arabidopsis thaliana* GSK3-like kinases activates brassinosteroid signaling. *Chem. Biol.* **16**:594–604.
- Delaney, T.P., Uknes, S., Vernooij, B., Friedrich, L., Weymann, K., Negrotto, D., Gaffney, T., Gut-Rella, M., Kessmann, H., Ward, E., et al.** (1994). A central role of salicylic acid in plant disease resistance. *Science* **266**:1247–1250.
- Fan, M., Bai, M.Y., Kim, J.G., Wang, T., Oh, E., Chen, L., Park, C.H., Son, S.H., Kim, S.K., Mudgett, M.B., et al.** (2014). The bHLH transcription factor HBI1 mediates the trade-off between growth and pathogen-associated molecular pattern-triggered immunity in *Arabidopsis*. *Plant Cell* **26**:828–841.
- Feys, B.J., Moisan, L.J., Newman, M.A., and Parker, J.E.** (2001). Direct interaction between the *Arabidopsis* disease resistance signaling proteins, EDS1 and PAD4. *EMBO J.* **20**:5400–5411.
- Feys, B.J., Wiermer, M., Bhat, R.A., Moisan, L.J., Medina-Escobar, N., Neu, C., Cabral, A., and Parker, J.E.** (2005). *Arabidopsis* SENESENCE-ASSOCIATED GENE101 stabilizes and signals within an ENHANCED DISEASE SUSCEPTIBILITY1 complex in plant innate immunity. *Plant Cell* **17**:2601–2613.
- Fu, Z.Q., and Dong, X.N.** (2013). Systemic acquired resistance: turning local infection into global defense. *Annu. Rev. Plant Biol.* **64**:839–863.
- Gampala, S.S., Kim, T.W., He, J.X., Tang, W., Deng, Z., Bai, M.Y., Guan, S., Lalonde, S., Sun, Y., Gendron, J.M., et al.** (2007). An essential role for 14-3-3 proteins in brassinosteroid signal transduction in *Arabidopsis*. *Dev. Cell* **13**:177–189.
- Gantner, J., Ordon, J., Kretschmer, C., Guerois, R., and Stuttmann, J.** (2019). An EDS1-SAG101 complex is essential for TNL-mediated immunity in *Nicotiana benthamiana*. *Plant Cell* **31**:2456–2474.
- Greene, G.H., and Dong, X.** (2018). To grow and to defend. *Science* **361**:976–977.
- He, J.X., Gendron, J.M., Sun, Y., Gampala, S.S.L., Gendron, N., Sun, C.Q., and Wang, Z.Y.** (2005). BZR1 is a transcriptional repressor with dual roles in brassinosteroid homeostasis and growth responses. *Science* **307**:1634–1638.
- He, J.X., Gendron, J.M., Yang, Y., Li, J., and Wang, Z.Y.** (2002). The GSK3-like kinase BIN2 phosphorylates and destabilizes BZR1, a positive regulator of the brassinosteroid signaling pathway in *Arabidopsis*. *Proc. Natl. Acad. Sci. U S A* **99**:10185–10190.
- Heidrich, K., Wirthmueller, L., Tasset, C., Pouzet, C., Deslandes, L., and Parker, J.E.** (2011). *Arabidopsis* EDS1 connects pathogen effector recognition to cell compartment-specific immune responses. *Science* **334**:1401–1404.
- Hinsch, M., and Staskawicz, B.** (1996). Identification of a new *Arabidopsis* disease resistance locus, RPS4, and cloning of the corresponding avirulence gene, *avrRps4*, from *Pseudomonas syringae* pv. *psis*. *Mol. Plant Microbe Interact.* **9**:55–61.
- Huh, S.U., Cevik, V., Ding, P., Duxbury, Z., Ma, Y., Tomlinson, L., Sarris, P.F., and Jones, J.D.G.** (2017). Protein-protein interactions in the RPS4/RRS1 immune receptor complex. *PLoS Pathog.* **13**:e1006376.
- Huot, B., Yao, J., Montgomery, B.L., and He, S.Y.** (2014). Growth-defense tradeoffs in plants: a balancing act to optimize fitness. *Mol. Plant* **7**:1267–1287.
- International Wheat Genome Sequencing Consortium., Appels, R., Eversole, K., Feuillet, C., Keller, B., Rogers, J., Pozniak, C.J., Choulet, F., Distelfeld, A., Poland, J., et al.** (2018). Shifting the

BZR1-EDS1 regulates plant growth and defense

Molecular Plant

- limits in wheat research and breeding using a fully annotated reference genome. *Science* **361**:eaar7191.
- Jimenez-Gongora, T., Kim, S.K., Lozano-Duran, R., and Zipfel, C.** (2015). Flg22-triggered immunity negatively regulates key BR biosynthetic genes. *Front. Plant Sci.* **6**:981.
- Jones, J.D., and Dangl, J.L.** (2006). The plant immune system. *Nature* **444**:323–329.
- Kang, S., Yang, F., Li, L., Chen, H., Chen, S., and Zhang, J.** (2015). The *Arabidopsis* transcription factor BRASSINOSTEROID INSENSITIVE1-ETHYL METHANESULFONATE- SUPPRESSOR1 is a direct substrate of MITOGEN-ACTIVATED PROTEIN KINASE6 and regulates immunity. *Plant Physiol.* **167**:1076–1086.
- Karasov, T.L., Chae, E., Herman, J.J., and Bergelson, J.** (2017). Mechanisms to mitigate the trade-off between growth and defense. *Plant Cell* **29**:666–680.
- Kim, T.W., and Wang, Z.Y.** (2010). Brassinosteroid signal transduction from receptor kinases to transcription factors. *Annu. Rev. Plant Biol.* **61**:681–704.
- Kinoshita, T., Cano-Delgado, A., Seto, H., Hiranuma, S., Fujioka, S., Yoshida, S., and Chory, J.** (2005). Binding of brassinosteroids to the extracellular domain of plant receptor kinase BRI1. *Nature* **433**:167–171.
- Kondo, Y., Ito, T., Nakagami, H., Hirakawa, Y., Saito, M., Tamaki, T., Shirasu, K., and Fukuda, H.** (2014). Plant GSK3 proteins regulate xylem cell differentiation downstream of TDF-TDR signalling. *Nat. Commun.* **5**:3504.
- Kono, A., and Yin, Y.** (2020). Updates on BES1/BZR1 regulatory networks coordinating plant growth and stress responses. *Front. Plant Sci.* **11**:617162.
- Le Roux, C., Huet, G., Jauneau, A., Camborde, L., Tremousaygue, D., Kraut, A., Zhou, B., Levailant, M., Adachi, H., Yoshioka, H., et al.** (2015). A receptor pair with an integrated decoy converts pathogen disabling of transcription factors to immunity. *Cell* **161**:1074–1088.
- Li, J., and Chory, J.** (1997). A putative leucine-rich repeat receptor kinase involved in brassinosteroid signal transduction. *Cell* **90**:929–938.
- Li, J., Wen, J., Lease, K.A., Doke, J.T., Tax, F.E., and Walker, J.C.** (2002). BAK1, an *Arabidopsis* LRR receptor-like protein kinase, interacts with BRI1 and modulates brassinosteroid signaling. *Cell* **110**:213–222.
- Li, Y., Yang, Y., Hu, Y., Liu, H., He, M., Yang, Z., Kong, F., Liu, X., and Hou, X.** (2019). DELLA and EDS1 form a feedback regulatory module to fine-tune plant growth-defense tradeoff in *Arabidopsis*. *Mol. Plant* **12**:1485–1498.
- Liao, K., Peng, Y., Yuan, L., Dai, Y., Chen, Q., Yu, L., Bai, M., Zhang, W., Xie, L., and Xiao, S.** (2020). Brassinosteroids antagonize jasmonate-activated plant defense responses through BRI1-EMS-SUPPRESSOR1 (BES1). *Plant Physiol.* **182**:1066–1082.
- Lozano-Duran, R., Macho, A.P., Boutrot, F., Segonzac, C., Somssich, I.E., and Zipfel, C.** (2013). The transcriptional regulator BZR1 mediates trade-off between plant innate immunity and growth. *eLife* **2**:e00983.
- Mackey, D., Belkhadir, Y., Alonso, J.M., Ecker, J.R., and Dangl, J.L.** (2003). *Arabidopsis* RIN4 is a target of the type III virulence effector AvrRpt2 and modulates RPS2-mediated resistance. *Cell* **112**:379–389.
- Mackey, D., Holt, B.F., Wiig, A., and Dangl, J.L.** (2002). RIN4 interacts with *Pseudomonas syringae* type III effector molecules and is required for RPM1-mediated resistance in *Arabidopsis*. *Cell* **108**:743–754.
- Malinovsky, F.G., Batoux, M., Schwessinger, B., Youn, J.H., Stransfeld, L., Win, J., Kim, S.K., and Zipfel, C.** (2014). Antagonistic regulation of growth and immunity by the *Arabidopsis* basic helix-loop-helix transcription factor homolog of brassinosteroid enhanced expression2 interacting with increased leaf inclination1 binding bHLH1. *Plant Physiol.* **164**:1443–1455.
- Mou, Z., Fan, W.H., and Dong, X.N.** (2003). Inducers of plant systemic acquired resistance regulate NPR1 function through redox changes. *Cell* **113**:935–944.
- Noguchi, T., Fujioka, S., Choe, S., Takatsuto, S., Yoshida, S., Yuan, H., Feldmann, K.A., and Tax, F.E.** (1999). Brassinosteroid-insensitive dwarf mutants of *Arabidopsis* accumulate brassinosteroids. *Plant Physiol.* **121**:743–752.
- Nolan, T., Vukašinović, N., Liu, D., Russinova, E., and Yin, Y.** (2020). Brassinosteroids: multidimensional regulators of plant growth, development, and stress responses. *Plant Cell* **32**:295–318.
- Parker, J.E., Holub, E.B., Frost, L.N., Falk, A., Gunn, N.D., and Daniels, M.J.** (1996). Characterization of eds1, a mutation in *Arabidopsis* suppressing resistance to *Peronospora parasitica* specified by several different RPP genes. *Plant Cell* **8**:2033–2046.
- Pieterse, C.M.J., Van der Does, D., Zamioudis, C., Leon-Reyes, A., and Van Wees, S.C.M.** (2012). Hormonal modulation of plant immunity. *Annu. Rev. Cell Dev. Biol.* **28**:489–521.
- Pike, S., Gassmann, W., and Su, J.** (2019). Generating transgenic *Arabidopsis* plants for functional analysis of pathogen effectors and corresponding R proteins. *Methods Mol. Biol.* **1991**:199–206.
- Rietz, S., Stamm, A., Malonek, S., Wagner, S., Becker, D., Medina-Escobar, N., Vlot, A.C., Feys, B.J., Niefind, K., and Parker, J.E.** (2011). Different roles of enhanced disease susceptibility1 (EDS1) bound to and dissociated from phytoalexin deficient 4 (PAD4) in *Arabidopsis* immunity. *New Phytol.* **191**:107–119.
- Sarris, P.F., Duxbury, Z., Huh, S.U., Ma, Y., Segonzac, C., Sklenar, J., Derbyshire, P., Cevik, V., Rallapalli, G., Saucet, S.B., et al.** (2015). A plant immune receptor detects pathogen effectors that target WRKY transcription factors. *Cell* **161**:1089–1100.
- Sato, H., Mizoi, J., Tanaka, H., Maruyama, K., Qin, F., Osakabe, Y., Morimoto, K., Otori, T., Kusakabe, K., Nagata, M., et al.** (2014). *Arabidopsis* DPB3-1, a DREB2A interactor, specifically enhances heat stress-induced gene expression by forming a heat stress-specific transcriptional complex with NF-Y subunits. *Plant Cell* **26**:4954–4973.
- Saucet, S., Ma, Y., Sarris, P., Furzer, O., Sohn, K., and Jones, J.** (2015). Two linked pairs of *Arabidopsis* TNL resistance genes independently confer recognition of bacterial effector AvrRps4. *Nat. Commun.* **6**:6338.
- Sheen, J.** (2001). Signal transduction in maize and *Arabidopsis* mesophyll protoplasts. *Plant Physiol.* **127**:1466–1475.
- Sun, Y., Fan, X.Y., Cao, D.M., Tang, W., He, K., Zhu, J.Y., He, J.X., Bai, M.Y., Zhu, S., Oh, E., et al.** (2010). Integration of brassinosteroid signal transduction with the transcription network for plant growth regulation in *Arabidopsis*. *Dev. Cell* **19**:765–777.
- Tang, W., Yuan, M., Wang, R., Yang, Y., Wang, C., Osés-Prieto, J.A., Kim, T.W., Zhou, H.W., Deng, Z., Gampala, S.S., et al.** (2011). PP2A activates brassinosteroid-responsive gene expression and plant growth by dephosphorylating BZR1. *Nat. Cell Biol.* **13**:124–131.
- Tian, Y., Fan, M., Qin, Z., Lv, H., Wang, M., Zhang, Z., Zhou, W., Zhao, N., Li, X., Han, C., et al.** (2018). Hydrogen peroxide positively regulates brassinosteroid signaling through oxidation of the BRASSINAZOLE-RESISTANT1 transcription factor. *Nat. Commun.* **9**:1063.
- Walter, M., Chaban, C., Schütze, K., Batistic, O., Weckermann, K., Näge, C., Blazevic, D., Grefen, C., Schumacher, K., Oecking, C., et al.** (2004). Visualization of protein interactions in living plant cells using bimolecular fluorescence complementation. *Plant J.* **40**:428–438.

Molecular Plant

- Wang, J., Zhou, L., Shi, H., Chern, M., Yu, H., Yi, H., He, M., Yin, J., Zhu, X., Li, Y., et al.** (2018). A single transcription factor promotes both yield and immunity in rice. *Science* **361**:1026–1028.
- Wang, W., and Wang, Z.Y.** (2014). At the intersection of plant growth and immunity. *Cell Host Microbe* **15**:400–402.
- Wang, W., Ye, R., Xin, Y., Fang, X., Li, C., Shi, H., Zhou, X., and Qi, Y.** (2011). An importin beta protein negatively regulates microRNA activity in *Arabidopsis*. *Plant Cell* **23**:3565–3576.
- Wang, Z.P., Xing, H.L., Dong, L., Zhang, H.Y., Han, C.Y., Wang, X.C., and Chen, Q.J.** (2015). Egg cell-specific promoter-controlled CRISPR/Cas9 efficiently generates homozygous mutants for multiple target genes in *Arabidopsis* in a single generation. *Genome Biol.* **16**:144.
- Wang, Z.Y., Nakano, T., Gendron, J., He, J., Chen, M., Vafeados, D., Yang, Y., Fujioka, S., Yoshida, S., Asami, T., et al.** (2002). Nuclear-localized BZR1 mediates brassinosteroid-induced growth and feedback suppression of brassinosteroid biosynthesis. *Dev. Cell* **2**:505–513.
- Wildermuth, M.C., Dewdney, J., Wu, G., and Ausubel, F.M.** (2001). Isochorismate synthase is required to synthesize salicylic acid for plant defence. *Nature* **414**:562–565.
- Wirthmueller, L., Zhang, Y., Jones, J., and Parker, J.** (2007). Nuclear accumulation of the *Arabidopsis* immune receptor RPS4 is necessary for triggering EDS1-dependent defense. *Curr. Biol.* **17**:2023–2029.
- Xu, G., Yuan, M., Ai, C., Liu, L., Zhuang, E., Karapetyan, S., Wang, S., and Dong, X.** (2017). uORF-mediated translation allows engineered plant disease resistance without fitness costs. *Nature* **545**:491–494.
- Yan, Z., Zhao, J., Peng, P., Chihara, R.K., and Li, J.** (2009). BIN2 functions redundantly with other *Arabidopsis* GSK3-like kinases to regulate brassinosteroid signaling. *Plant Physiol.* **150**:710–721.
- Yu, X., Li, L., Zola, J., Aluru, M., Ye, H., Foudree, A., Guo, H., Anderson, S., Aluru, S., Liu, P., et al.** (2011). A brassinosteroid transcriptional network revealed by genome-wide identification of BES1 target genes in *Arabidopsis thaliana*. *Plant J.* **65**:634–646.
- Yu, M., Zhao, Z., and He, J.** (2018). Brassinosteroid signaling in plant-microbe interactions. *Int. J. Mol. Sci.* **19**:4091.
- Zhang, J., and Zhou, J.M.** (2010). Plant immunity triggered by microbial molecular signatures. *Mol. Plant* **3**:783–793.
- Zhang, Y., Li, B., Xu, Y., Li, H., Li, S., Zhang, D., Mao, Z., Guo, S., Yang, C., Weng, Y., et al.** (2013). The cyclophilin CYP20-2 modulates the conformation of BRASSINAZOLE-RESISTANT1, which binds the promoter of FLOWERING LOCUS D to regulate flowering in *Arabidopsis*. *Plant Cell* **25**:2504–2521.
- Tang, X., Zhuang, Y., Qi, G., Wang, D., Liu, H., Wang, K., Chai, G., Zhou, G., et al.** (2015). Poplar PdMYB221 is involved in the direct and indirect regulation of secondary wall biosynthesis during wood formation. *Sci Rep* **5**, 12240. <https://doi.org/10.1038/srep12240>.

BZR1-EDS1 regulates plant growth and defense